Surveys in Geophysics (2005) 26:545–592
DOI 10.1007/s10712-005-1758-7

MAGNETIC PULSATIONS: THEIR SOURCES AND RELATION TO SOLAR WIND AND GEOMAGNETIC ACTIVITY

ROBERT L. MCPHERRON
Institute of Geophysics and Planetary Physics, University of California Los Angeles, Los Angeles, CA, 90095-1567, U.S.A E-mail: rmcpherron@igpp.ucla.edu

(Received 1 February 2003; accepted 25 May 2004)

Abstract. Ultra low frequency (ULF) waves incident on the Earth are produced by processes in the magnetosphere and solar wind. These processes produce a wide variety of ULF hydromagnetic wave types that are classified on the ground as either Pi or Pc pulsations (irregular or continuous). Waves of different frequencies and polarizations originate in different regions of the magnetosphere. The location of the projections of these regions onto the Earth depends on the solar wind dynamic pressure and magnetic field. The occurrence of various waves also depends on conditions in the solar wind and in the magnetosphere. Changes in orientation of the interplanetary magnetic field or an increase in solar wind velocity can have dramatic effects on the type of waves seen at a particular location on the Earth. Similarly, the occurrence of a magnetospheric substorm or magnetic storm will affect which waves are seen. The magnetosphere is a resonant cavity and waveguide for waves that either originate within or propagate through the system. These cavities respond to broadband sources by resonating at discrete frequencies. These cavity modes couple to field line resonances that drive currents in the ionosphere. These currents reradiate the energy as electromagnetic waves that propagate to the ground. Because these ionospheric currents are localized in latitude there are very rapid variations in wave phase at the Earth's surface. Thus it is almost never correct to assume that plane ULF waves are incident on the Earth from outer space. The properties of ULF waves seen at the ground contain information about the processes that generate them and the regions through which they have propagated. The properties also depend on the conductivity of the Earth underneath the observer. Information about the state of the solar wind and the magnetosphere distributed by the NOAA Space Disturbance Forecast Center can be used to help predict when certain types and frequencies of waves will be observed. The study of ULF waves is a very active field of space research and much has yet to be learned about the processes that generate these waves.

Keywords: cavity modes, file line resonances, MHD, magnetic storm, magnetosphere, pulsations, solar wind, substorm

1. Introduction and fundamentals

1.1 What are micropulsations, magnetic pulsations, and ULF waves?

Magnetic micropulsation is the name originally given to low frequency oscillations of the Earth's magnetic field. The name represents the manner in

which these oscillations were discovered through observation of the end of a very long compass needle with a microscope. The following quote from Chapman and Bartels (1962) is taken from one of the first published reports (about 1857) of such oscillations.

> "From the serrated appearance of the curves, it will be seen that a force tending to increase one of the elements[1] was generally followed after a short interval by one of the opposite description, and vice versa. The exertion of the disturbing force was thus of a throbbing or pulsatory character. The interval of time between two of these minute pulsations may be said to have varied from half a minute, or the smallest observable portion of time, up to four or five minutes. This pulsatory character of the disturbing force agrees well with the nature of its action on telegraphic wires, in which observers have noticed that the polarity of the current changes very frequently."

The waveform of these waves was eventually recorded by reflecting from a mirror on the needle a light beam onto a photographic film. An example recording is shown in Figure 1. The peak-to-peak amplitude of the waves in this figure is about 40 nT and their period is about 2 min. As more was learned about the waves the prefix "micro" was dropped and these oscillations became known as magnetic pulsations. More recently the signals were renamed again as ultra low frequency (ULF) waves. The international definition of this portion of the electromagnetic spectrum is any wave occurring in the frequency band from 1 mHz to 1 Hz (1000 to 1 s period).

1.2 Classification of ULF waves

In 1963, an IAGA committee classified ULF waves using a system dependent on waveform and wave period (Jacobs et al., 1964). Oscillations with quasi-sinusoidal waveform are called pulsations continuous (Pc). Those with waveforms that are more irregular are called pulsations irregular (Pi). Each major type is subdivided into period bands that roughly isolate a specific type of pulsation. Today it is known that the limits of these bands are not precise, and that more than one process produces waves in a particular band. The definitions of these frequency bands are shown in Figure 2.

1.3 How are ULF waves created?

ULF waves are created by a variety of processes in a magnetized plasma. Plasma is the name given to highly ionized gases threaded by a magnetic field.

[1] i.e. components of the geomagnetic field

When the collision frequency in a plasma is sufficiently low, the charged particles simply gyrate around the magnetic field and travel along it. Any force that moves the charged particles also moves the magnetic field and vice versa. In this situation the field and plasma are "frozen together". This

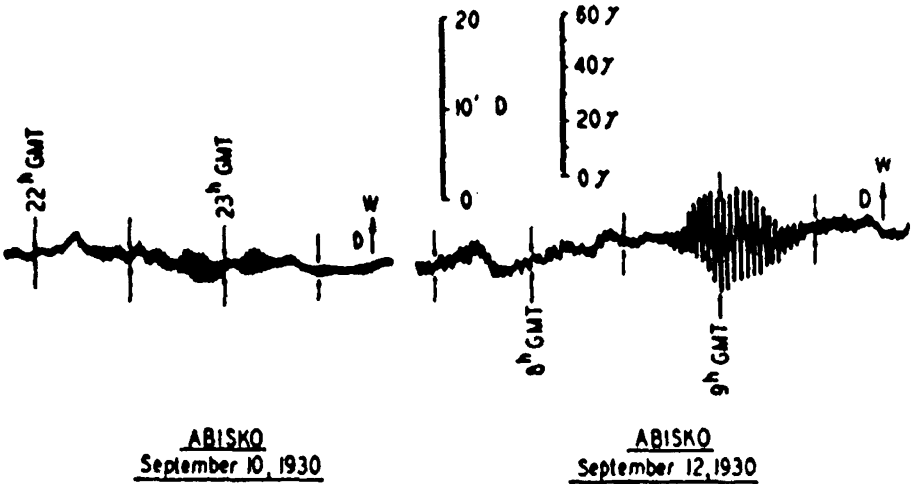

Figure 1. An example of a photographic recording of magnetic oscillations of a compass needle in northern Sweden. Vertical lines denote half hour intervals. The vertical scale is shown in units of both minutes of arc and nanoTesla (nT), previously termed γ . The pulsation packet at about 0900 UT (i.e. Universal Time, or Greenwich Mean Time) is called a giant pulsation (Portion of figure 11 (p.351) from "Geomagnetism, Volume 1: Geomagnetic and related phenomena" by permission of Oxford University Press).

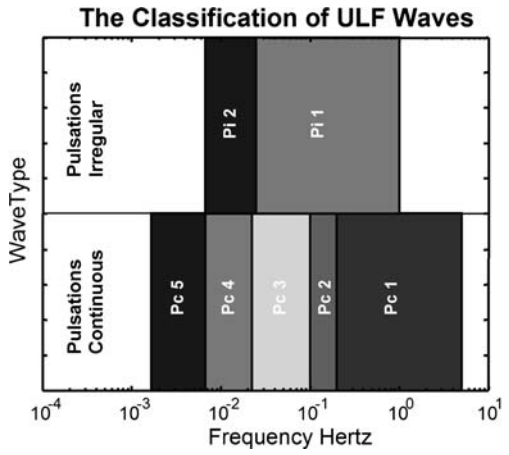

Irregular Pulsations

Class	Low edge Period (s)	High edge Period (s)
Pi 2	150	45
Pi 1	45	1

Continuous Pulsations

Class	Low edge Period (s)	High edge Period (s)
Pc 5	600	150
Pc 4	150	45
Pc 3	45	10
Pc 2	10	5
Pc 1	5	0.2

Figure 2. ULF waves are classified into two types: pulsations continuous (Pc) and pulsations irregular (Pi). Each type is subdivided into frequency bands roughly corresponding to distinct phenomena (Jacobs et al., 1964).

concept enabled Hannes Alfvén to describe a simple process that creates a low frequency wave that propagates along a magnetic field line. He received the Nobel Prize for this discovery and the wave he described is now called the Alfvén wave.

Alfvén's model for wave generation is summarized in Figure 3 (Alfvén and Falthammar, 1963). Consider an infinite volume of fully ionized hydrogen. As shown in the perspective view of panel (a), imagine that a force is applied to the plasma perpendicular to the magnetic field flux density $\boldsymbol{B}$ displacing a rectangular section of plasma with velocity $\boldsymbol{V}$. As the charges begin to move they experience a Lorentz force $\boldsymbol{F} = q(\boldsymbol{V} \times \boldsymbol{B})$, where q is the charge in Coulombs. The electrons move to the left side of the moving slab, and the protons to the right side as illustrated in the top view panel (b). This polarization of the charges creates an electric field $\boldsymbol{E}$ orthogonal to both $\boldsymbol{V}$ and $\boldsymbol{B}$. If the slab were in a vacuum the charges would be trapped at the edges of the column and the force of the electric field would eventually stop any further transfer of charge. At this point the electric force would be equal and opposite to the Lorentz force so that $\boldsymbol{E} = -\boldsymbol{V} \times \boldsymbol{B}$. However, in a plasma the charges can flow through the surrounding fluid in an attempt to neutralize the polarization. This charge motion creates an electrical current density $\boldsymbol{J}$ as shown in the end view of panel (c). As this current flows across the magnetic field above and below the moving slab it exerts a force on the gas, $\boldsymbol{F} = \boldsymbol{J} \times \boldsymbol{B}$.

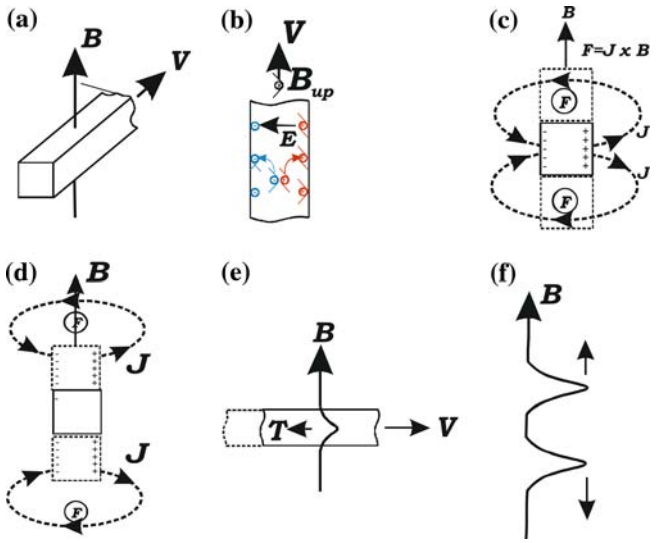

Figure 3. The creation of an Alfvén wave by displacing a slab of plasma threaded by a magnetic field. Panels (a) to (f) show successive steps in the production of a pair of pulses that propagate along a magnetic field line – see text for a full discussion (after Figures 3.1–3.3 in Alfvén and Falthammar, 1963).

This force is in the same direction as the initial motion of the slab. Consequently, the plasma above and below begins to move.

The same argument can now be applied to these two moving slabs. They become polarized, driving currents that cause slabs further above and below the initial slab to start moving as seen in panel (d). Clearly, the initial disturbance is propagating in both directions along the magnetic field away from the initial disturbance. As illustrated in the side view of panel (e) the displacement of the slab distorts the magnetic field that is frozen into the plasma. As the field bends, tension develops creating a restoring force that brings the slab to a stop and then returns it towards its initial location. As this happens the moving slabs above and below the initial slab distort the field line in the same way so that two pulses appear to propagate away from the origin. These pulses are Alfvén waves.

1.4 Solutions of the MHD wave equation

The Alfvén wave is only one of the wave modes that can propagate in a plasma. Maxwell's equations for the electric and magnetic fields have two independent solutions. In addition, a gas also supports sound waves, propagating pressure (or density) fluctuations. In a magnetized plasma the two electromagnetic waves are coupled to the sound wave by the "frozen in" magnetic field, and there are three solutions to the basic equations. A low frequency approximation to the basic equations is called magnetohydrodynamics (MHD). The wave solutions to these equations are called MHD waves.

To understand low frequency waves in space plasmas one must begin with the basic equations of MHD which include three fluid equations, four Maxwell's equations, and Ohm's law. The fluid equations are the following:

$$\begin{aligned} &\tfrac{\partial}{\partial t}\rho + \nabla\cdot(\rho \boldsymbol{V}) = 0 && \text{– Equation of continuity}\\ &\tfrac{\partial}{\partial t}\boldsymbol{V} = -\nabla p + \boldsymbol{J}\times\boldsymbol{B} && \text{– Equation of motion}\\ &\tfrac{p}{\rho^{\gamma}} = \text{constant} && \text{– Equation of state} \end{aligned} \tag{1}$$

In these equations ρ is the plasma density, $\boldsymbol{V}$ is the velocity, p is the pressure, $\boldsymbol{J}$ is the current density, $\boldsymbol{B}$ is the magnetic flux density, and γ is the ratio of specific heats.

Maxwell's equations are:

$$\begin{aligned} &\nabla\cdot\boldsymbol{E} = \rho/\varepsilon_0 \quad \nabla\times\boldsymbol{E} = -\frac{\partial}{\partial t}\boldsymbol{B}\\ &\nabla\cdot\boldsymbol{B} = 0 \quad \nabla\times\boldsymbol{B} = \mu_0\boldsymbol{J} + \varepsilon_0\mu_0\frac{\partial}{\partial t}\boldsymbol{E}. \end{aligned} \tag{2}$$

Here $\boldsymbol{E}$ is the electric field, and ε_0 and μ_0 are, respectively, the permittivity and permeability of free space.

At the frequency of ULF waves the polarization current can be ignored and the last term in Ampere's law is $\partial \boldsymbol{E}/\partial t \approx 0$ dropped. Generally we assume an electrically neutral plasma, with $\rho = 0$. Finally, Ohm's law in the frame in which the plasma velocity is measured can be written:

$$\boldsymbol{J} = \sigma(\boldsymbol{E} + \boldsymbol{V} \times \boldsymbol{B}) \tag{3}$$

where σ is the electrical conductivity.

To study the properties of ULF waves assume that the background velocity of the plasma is zero so that $\boldsymbol{V} = 0 + \boldsymbol{V}'$. Then write the magnetic field as the sum of a background field and a perturbation $\boldsymbol{B} = \boldsymbol{B}_0 + \boldsymbol{B}'$. Similarly write the density and pressure in terms of background values and small perturbations $\rho = \rho_0 + \rho'$ and $p = p_0 + p'$. Substitute these expressions into the preceding equations and ignore terms of second order in the perturbations. The result after several substitutions and algebraic manipulation is a set of four equations.

$$\begin{aligned}
&\rho_0 \frac{\partial}{\partial t} \boldsymbol{V}' = -\nabla p + \frac{1}{\mu_0}[(\nabla \times \boldsymbol{B}') \times \boldsymbol{B}_0] \\
&\nabla p = \nabla \rho = \gamma \frac{p_0}{\rho_0} \nabla \rho' \\
&\frac{\partial}{\partial t} \rho' + \rho_0 (\nabla \cdot \boldsymbol{V}') = 0 \\
&\frac{\partial}{\partial t} \boldsymbol{B}' = (\boldsymbol{B}_0 \cdot \nabla) \boldsymbol{V}' = \boldsymbol{B}_0 (\nabla \cdot \boldsymbol{V}').
\end{aligned} \tag{4}$$

Nowassume that all quantities oscillate proportionally to the quantity $e^{i\vec{k} \cdot \vec{r} - i\omega x}$ where $\boldsymbol{k}$ is the wavenumber and ω is the angular frequency of the wave, and $\boldsymbol{r}$ is the position vector. Again substitute and simplify to obtain a set of four algebraic equations. These four equations can be solved obtaining a single vector equation for the velocity perturbation of the plasma. This equation is

$$\begin{aligned}
\omega^2 \boldsymbol{V}' - \gamma \frac{p_0}{\rho_0} \boldsymbol{k}(\boldsymbol{k} \cdot \boldsymbol{V}') - \frac{1}{\mu_0 \rho_0} \{ & B_0^2 \boldsymbol{k}(\boldsymbol{k} \cdot \boldsymbol{V}') - \boldsymbol{B}_0 (\boldsymbol{k} \cdot \boldsymbol{V}')(\boldsymbol{k} \cdot \boldsymbol{B}_0) \\
& - \boldsymbol{k}(\boldsymbol{k} \cdot \boldsymbol{B}_0)(\boldsymbol{B}_0 \cdot \boldsymbol{V}') + (\boldsymbol{k} \cdot \boldsymbol{B}_0)^2 \boldsymbol{V}' = 0.
\end{aligned} \tag{5}$$

This equation can be simplified by introducing a special coordinate system and two characteristic velocities. First note that $s^2 = \gamma(p_0/\rho_0)$ is the square of the sound speed. Also the square of the Alfvén velocity is defined as

$V_A{}^2 = B_0{}^2/\mu\rho_0$. Now choose a coordinate system in which the magnetic field $\boldsymbol{B}_0$ lies along the z axis, and the wavenumber $\boldsymbol{k} = k\hat{\boldsymbol{n}}$ with $\hat{\boldsymbol{n}}$ the direction of propagation, lies in the y–z plane along the unit vector $\hat{\boldsymbol{n}}$ at an angle θ to the z axis.

These choices considerably simplify the equation which becomes

$$\left(\frac{\omega^2}{k^2} - V_A^2\cos^2\theta\right)\boldsymbol{V}' - \left[(s^2 + V_A^2)(\hat{\boldsymbol{n}}\cdot\boldsymbol{V}') - V_A^2(\hat{\boldsymbol{n}}\cdot\hat{\boldsymbol{z}})(\hat{\boldsymbol{z}}\cdot\boldsymbol{V}')\right]\hat{\boldsymbol{n}} + V_A^2(\hat{\boldsymbol{n}}\cdot\hat{\boldsymbol{z}})(\hat{\boldsymbol{n}}\cdot\boldsymbol{V}')\hat{\boldsymbol{z}} = 0. \tag{6}$$

Note that this is a vector equation corresponding to the three elements of the plasma velocity $\boldsymbol{V}'$. In matrix form this equation appears much simpler.

$$\begin{pmatrix} \left(\frac{\omega^2}{k^2} - V_A^2\cos^2\theta\right) & 0 & 0 \\ 0 & \left(\frac{\omega^2}{k^2} - s^2\sin^2\theta - V_A^2\right) & -s^2\sin\theta\cos\theta \\ 0 & -s^2\sin\theta\cos\theta & \left(\omega^2 2 - s^2\cos^2\theta\right) \end{pmatrix} \begin{pmatrix} V_x' \\ V_y' \\ V_z' \end{pmatrix} = 0. \tag{7}$$

This set of three homogenous equations cannot be satisfied with arbitrary $\boldsymbol{V}'$. For example, suppose V_x' is not zero. Then the first equation requires that the term in the upper left corner of the matrix is zero. This implies that the phase velocity of the wave is $u^2 = (\omega/k)^2 = V_A^2\cos^2\theta$. If we substitute this value of phase velocity into the next two equations it can be shown that the only possible solution is for $V_y' = V_z' = 0$. On the other hand, if we assume $V_x' = 0$ then we can solve the second set of equations for the ratio V_y'/V_z' provided that the square of the phase velocity takes on one of two different values obtained from the quadratic equation defined by the determinant of the four lower right terms in the matrix. Depending on which solution is used one obtains a different ratio of y and z components.

Thus there are three solutions to this set of equations corresponding to three different modes of wave propagation. The first wave is the Alfvén wave. It has only an x-component of the perturbation velocity orthogonal to the plane containing the ambient field and the direction of propagation. The other two wave modes are coupled. One has a speed that is fast compared to the Alfvén wave, and the other a speed that is slow. The angular dependence of these waves' speeds is illustrated below.

There is a variety of names for the three MHD waves, but the most common are fast, intermediate, and slow waves. These names are based on the speed of the wave along the magnetic field. The fast wave is a combi-

nation of pressure and field fluctuations. When the fast wave propagates perpendicular to the background field it is seen as alternating compressions and rarefactions of both the field and density. The intermediate speed wave is the Alfvén wave just described. It consists of bends in the field that do not change the density. The slow wave is closest to being a pure sound wave. Each of these waves has unique polarization properties with the electric, magnetic, and plasma velocity fluctuations being oriented in different directions relative to the direction of wave propagation and background field.

The dependence of wave speed on direction of propagation for the three wave modes is shown in Figure 4. The fast mode and Alfvén mode propagate with the Alfvén velocity along the field. This velocity is given by $V_A = \sqrt{B^2/\mu_0\rho}$ where B is the field strength and ρ the plasma density. Perpendicular to the field the fast mode speed is a combination of the Alfvén and sound speeds, $c_{\rm ms} = \sqrt{c_s^2 + v_A^2}$. The Alfvén mode does not propagate in this perpendicular direction. Parallel to the field the slow mode moves at the sound speed $c_s = \sqrt{\gamma k_{\rm B} T/m_i}$ and, like the Alfvén wave, does not propagate perpendicular to the field.

In general, the ULF waves seen at the ground originate in space as either fast mode, or intermediate mode, or a combination of the two. They propagate along or across the magnetic field until they reach the ionosphere. At

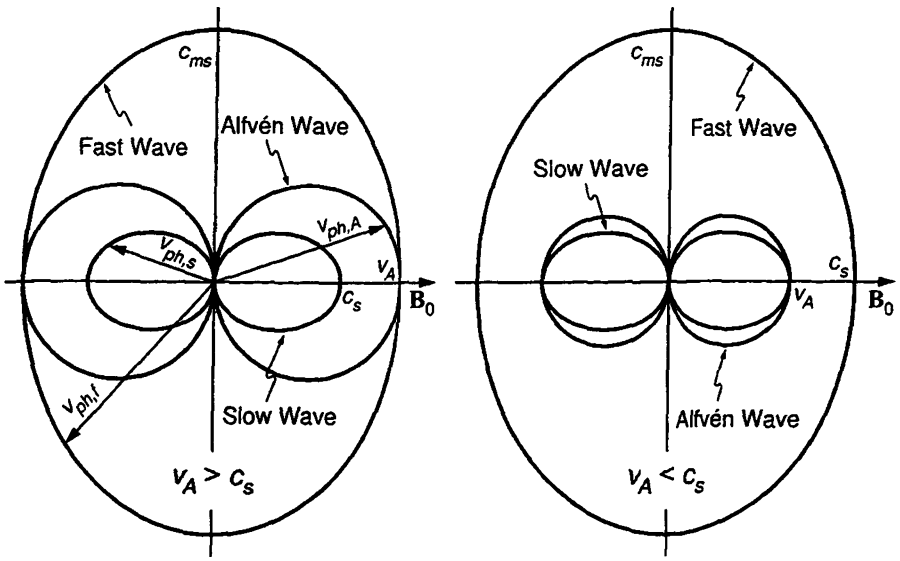

Figure 4. The diagram shows the speed of the fast, intermediate (Alfvén), and slow waves as a function of the angle of propagation relative to the background field B_0. V_A is the Alfvén speed, c_s is the sound speed, and $c_{\rm ms}$ is the magnetosonic speed, a combination of the Alfvén and sound speed (Baumjohann and Treumann, 1996). For propagation at an angle to the magnetic field, $V_{\rm ph}$ shows the phase velocity of different wave modes.

the ionosphere they drive electrical currents that radiate pure electromagnetic waves into the neutral atmosphere. Thus magnetic pulsations measured on the ground are MHD waves converted to purely electromagnetic waves in the ionosphere.

ULF waves measured on the ground are produced in various regions of the magnetosphere by a variety of physical processes. To understand what type of waves will be seen at particular latitudes one must know which region of the magnetosphere the local field line passes through. Unfortunately, the magnetosphere is highly dynamic and the magnetic projections of these regions change with the level of magnetic activity. There are two main solar wind parameters that determine the locations of these regions, the dynamic pressure, ρV^2, and the rate of transport of southward magnetic flux, VB_s. Increases in dynamic pressure compress the magnetosphere, shrinking its size. Southward magnetic field erodes magnetic flux from the day side, allowing the solar wind to transport this flux to the night side where it accumulates in the lobes of the magnetic tail. All of the boundaries and regions play important roles in determining the type of ULF waves seen on the ground (McPherron, 1991; McPherron et al., 1973).

1.5 An equatorial view of the solar wind and magnetosphere

Figure 5 shows a geocentric solar magnetospheric (GSM) equatorial cross section of the magnetosphere for a low solar wind dynamic pressure of 0.8 nPa. The GSM coordinate system has an X axis always pointing to the Sun, a Y axis orthogonal to the plane of X and the Earth's dipole moment, and a Z axis perpendicular to X and Y. This system continuously rotates around the Sun vector to keep the dipole moment in the X–Z plane. The outer limit of the Earth's magnetic field is called the magnetopause. The magnetopause is a layer of current that confines the Earth's field inside the boundary. At the nose of the magnetosphere this boundary is usually at a geocentric distance of about 10 Re. At the flanks, it is 15 Re away, and, far down the tail, it is at a distance of 25–30 Re from the center. Upstream of the magnetopause is the bow shock. The shock is typically about 3 Re upstream of the magnetopause. The shock exists because the solar wind is typically moving at about eight times the speed of the fast mode wave, i.e. the solar wind is super magnetosonic. The shock must slow down the solar wind enough that fast waves travel faster than the flow so that they can carry pressure information upstream. The waves setup a pressure distribution Earthward of the shock that deflects the flow around the magnetopause.

On the nightside a thick layer of plasma separates the two lobes of the magnetic field (see Figure 6). In Figure 5 there is an inner edge to this sheet of plasma that roughly corresponds to the first closed drift path (in longitude) around the Earth for hot electrons from the tail. Inside this boundary is the

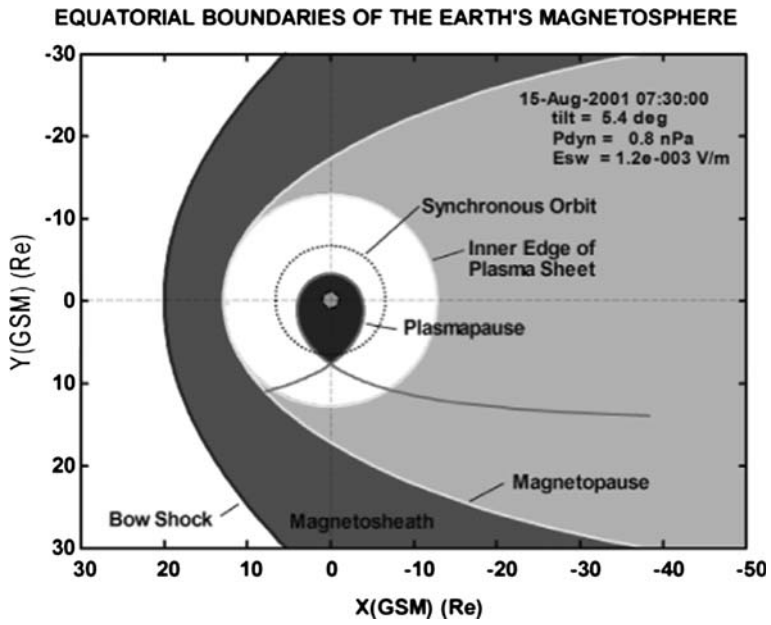

Figure 5. Model boundaries of various regions of the magnetosphere are projected into the GSM (see text) equatorial plane. They include the bow shock, magnetopause, plasmapause, and inner edge of the plasma sheet. The circle around the Earth at 6.6 Re is synchronous (or geostationary) orbit.

plasmapause, a sharp boundary in plasma density. The plasmapause, created by electric fields in the magnetosphere, is highly dynamic moving inward with increasing magnetic activity, and outward with decreasing activity. In a steady state the plasmapause is a separatrix between cold charged particle drift paths that are open to the magnetopause and those that are closed around the Earth. Cold particles from the ionosphere fill the plasmasphere. The extension of the separatrix into the tail is shown in the diagram.

1.6 A NOON-MIDNIGHT MERIDIAN VIEW OF THE MAGNETOSPHERE

The intersections of the various magnetospheric boundaries with the noon-midnight meridian plane are shown in Figure 6. This projection shows the shape of the Earth's magnetic field as distorted by its interaction with the solar wind. On the dayside the geomagnetic field typically ends at about 10 Re. The regions separating field lines that pass through the dayside equator, and those that are swept back into the tail, are called the northern and southern polar cusps. The cusps provide openings for particles and waves in the magnetosheath (the region between the bow shock and magnetopause) to enter the magnetosphere easily.

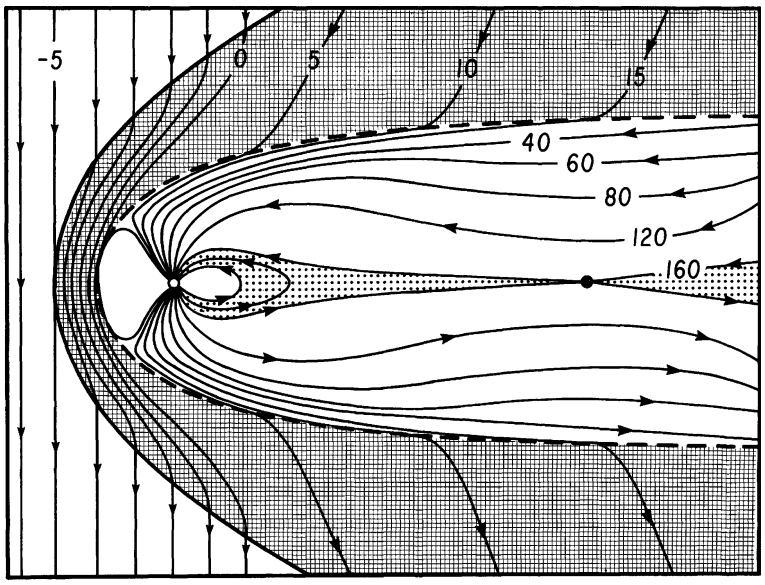

Figure 6. A projection of the magnetosphere into the noon-midnight meridian plane at equinox when the dipole axis is orthogonal to the Earth–Sun line. The Sun is to the left and the magnetic tail to the right. The dotted region behind the Earth along the Earth–Sun line is the plasma sheet. The bow shock, magnetopause, inner edge of the plasma sheet, upper and lower edges of the plasma sheet and the tail lobes are also depicted. Field lines in the solar wind are taken to be purely southward and interacting with the Earth's field producing a magnetic configuration open to the solar wind. The numbers show the time (in minutes) that the field line is at a particular place relative to time zero for a field line at the magnetopause to reconnect (Reproduced by permission of American Geophysical Union, McPherron et al., 1973).

Note that the magnetopause does not completely contain the geomagnetic field when the solar wind magnetic field is southward. This orientation allows the solar wind field to merge with the Earth's field at the nose, creating an 'X-line' field configuration. The solar wind then transports the interconnected field lines over the Earth's poles and stretches them into a long tail on the nightside. Far behind the Earth at the center of the tail is another X-line where the field lines come back together and "reconnect". The newly reconnected field lines then move up the tail towards the Sun, flowing around the Earth. Note that there are three types of field lines in this figure: solar wind field lines connected to the Sun; open field lines connected to the Sun at one end and to one polar region of the Earth at the other; closed field lines that connect to the Earth at each end. This field geometry projects disturbances in the magnetosphere onto the Earth.

1.7 Projection of the magnetosphere onto the Earth's surface

Figure 7 presents a north polar view of the Earth identifying various projected regions. Intuition based on the properties of the dipole field does not work well in this projection because of the extreme distortion of the outer parts of the magnetic field. A roughly circular region around the North magnetic pole is called the polar cap. Field lines from this region pass outward into the northern lobe of the magnetic tail. They eventually pass through the magnetopause, becoming solar wind field lines. Because these field lines are open to the solar wind, they provide easy access to certain types of charged particles coming from the Sun.

Equatorward of the polar cap is the auroral oval. On the nightside the auroral oval maps into the plasma sheet. The poleward edge of the nightside oval is generally assumed to be the last closed field line that connects to the distant X-line. The equatorward edge of the auroral oval maps to the inner edge of the plasma sheet. On the dayside the oval projects to the polar cusp,

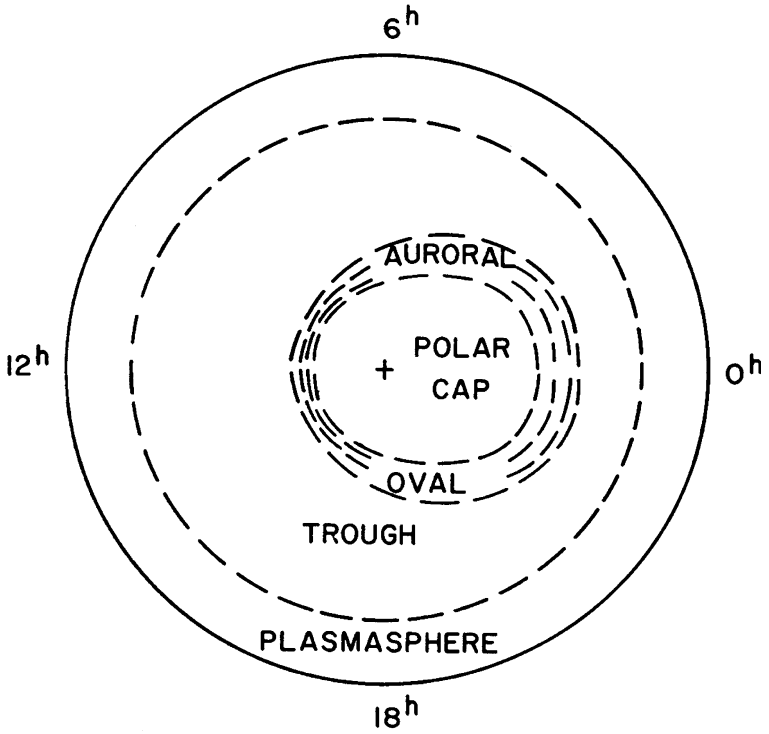

Figure 7. Projection of magnetospheric regions onto the Earth at different Local Times (LT). The cross denotes the magnetic pole. The polar cap is the region poleward of the auroral oval. The plasma trough is equatorward of the oval, but poleward of the plasmasphere (Vasyliunas, 1983).

the region where field lines normally crossing the equator on the dayside are swept back into the tail.

As mentioned earlier the Earth's magnetic field lines merge with a southward solar wind magnetic field at the nose of the magnetosphere and are then dragged over the polar caps. The feet of these field line move from noon to midnight across the polar cap, dragging the ionospheric plasma towards midnight. Eventually these open field lines reconnect at the distant X-line and flow sunward in the plasma sheet passing around the Earth. The feet of these field lines leave the polar cap and travel through the auroral oval dragging the ionospheric plasma. Depending on which side of the separatrix the field lines are on they will pass around either the dawn or dusk side of the Earth. This closed system of magnetospheric and ionospheric plasma flow is called magnetospheric and ionospheric convection.

Somewhat equatorward of the auroral oval is the projection of the plasmapause. Under quiet conditions the ionosphere equatorward of the plasmapause is shielded from the effects of convection.

2. Relation of ULF waves to magnetospheric substorms and magnetic storms

Many of the ULF waves generated internally in the magnetosphere are associated with either substorms or magnetic storms. The reason is that these processes create distributions of charged particle pressure, energy, and pitch angle that are unstable to the creation of various types of waves. To help understand the cause of ULF waves of internal origin we briefly describe these phenomena.

2.1 Magnetospheric substorm

The magnetospheric substorm is a systematic response of the magnetosphere to an increase in coupling between the solar wind and the Earth's magnetic field (McPherron, 1991). A substorm typically lasts around 3 h and occurs 3–6 times per day. During a substorm a large amount of energy is extracted from the solar wind and is dumped into the magnetosphere and ionosphere. The substorm is characterized by three phases: growth, expansion, and recovery. The growth phase begins when the solar wind magnetic field turns southward and magnetic reconnection begins at the subsolar magnetopause. Magnetic field lines of the solar wind merge with the Earth's field and are carried over the polar caps and stretched into a long tail behind the Earth. As open magnetic field lines accumulate in the tail lobes they exert increasing pressure on the plasma sheet causing it to thin. In reaction to the increased drag on the tail, the tail current moves earthward and strengthens to correspond to the increased magnetic field in

the lobes. At the same time, plasma and magnetic field begin to flow up the tail towards the X-line at the front of the magnetosphere to replace field lines removed by reconnection. This flow is diverted around both sides of the Earth creating a two-celled convection system within the magnetosphere. This process continues until the plasma sheet becomes too thin at midnight about 20 Re behind the Earth. A new X-line is created in a limited local time sector about 3 Re west of midnight (Nagai and Machida, 1998). This signals the beginning of the expansion phase. The duration of the growth phase is typically one hour.

During the growth phase the size of the polar cap grows as more magnetic field lines are connected to the solar wind. The open field lines enable the solar wind electric field that points from dawn to dusk to be transmitted to the ionosphere. The electric field drives a Pedersen current down field lines on the morning side, across the polar cap, and up field lines on the dusk side. In addition, some of the dawnside current flows equatorward to the plasmapause where it closes upward along field lines. This portion of the current continues around the nightside equator as a partial ring current. Near dusk and in the late afternoon it is diverted downward near the plasmapause, attaching to a poleward current in the dusk oval. The current merges with the current coming across the polar cap and flows out along field lines. This complex current system is nearly invisible on the ground! However, the electric field also drives a Hall current in the ionosphere. It flows along the auroral oval towards midnight. On the dawn side this portion of the current is called the westward electrojet. On the dusk side it is called the eastward electrojet. Near midnight the currents meet and flow poleward across the polar cap diverging into the electrojets at the dayside auroral oval. Magnetic disturbances seen on the ground during the growth phase are due to this DP-2 (disturbance polar-type 2) current system.

In the first stage of the expansion phase the X-line reconnects closed field lines in the plasma sheet creating a bubble of closed magnetic flux called a plasmoid (Baker et al., 1996). Eventually the reconnection reaches the last closed field lines that form the boundary of the plasma sheet. These field lines are normally connected to an inactive, distant X-line located beyond 100 Re down the tail. The second stage of the expansion begins when reconnection reaches open field lines in the lobe. At this time the plasmoid is no longer held to the Earth by closed field lines. It is ejected down the tail by a combination of forces including the time varying momentum of plasma injected in the bubble by reconnection in the first stage, the magnetic tension of field lines connected only to the solar wind and bent around the bubble, and the dynamic pressure of the flow from reconnection in the second stage.

Reconnection also drives plasma and magnetic flux earthward from the near-Earth X-line. As this flow impacts the inner magnetic field, it causes disturbances that project to the Earth at the equatorward edge of the auroral

oval near midnight. With time, more flow piles up in this region and a compression front moves backwards in the tail. The region earthward of this front projects to the ionosphere as a region of bright, active aurora. With time this region expands both poleward and azimuthally, creating what is called the auroral bulge. Some of the plasma flowing sunward from the X-line is diverted around the Earth. The pressure gradients, vorticity, and magnetic shear caused by this diversion create a field-aligned current (FAC) system called the substorm current wedge (Birn and Hesse, 1996). Current previously flowing across the tail close to the Earth is diverted down field lines on the morning side to flow westward across the bulge and close upward from the west side of the bulge. The ground magnetic disturbance associated with this current is called DP-1. This process continues for about 30–40 minutes until the X-line begins to move down the tail. This signals the beginning of the recovery phase

In the recovery phase the magnetosphere returns to its presubstorm configuration of field and plasma. Magnetic flux accumulated in the tail lobes is closed and returned to the dayside. The inner edge of the tail current moves more tailward; the plasma sheet thickens. The X-line retreats to about 100 Re and remains fixed at this location. Sporadic, weak bursts of reconnection at this line create poleward boundary intensifications in the auroral oval as flow bursts travel earthward from the reconnection site.

Many ULF waves are created by changes in fields and plasmas during substorms. The Pi 2 pulsations are related to flow bursts. Pi-1 may be created by some process in the topside Alfvénic resonator (Pilipenko et al., 2002). Intervals of pulsations of diminishing period (IPDP) are generated by protons energized and injected near midnight by the substorm expansion. As explained earlier convection preferentially energizes particles at large pitch angles setting up the conditions for instability. These protons also create Pc 4–5 waves near the dusk meridian through the drift-mirror instability. However, these waves are not seen on the ground because they have such small azimuthal wavelengths. Drifting electrons are precipitated in the early morning hours by some unknown process that causes patches of aurora pulsating with about 1–30 s period. The auroral torches are formed near midnight and drift eastward diverting current along field lines and creating ground fluctuations of long period (Ps 6).

2.2 Magnetic storms

A magnetic storm is an interval of several days duration during which there is a large reduction in the horizontal component of the geomagnetic field at the Earth's surface (Gonzalez et al., 1994). A classic magnetic storm begins with a sudden commencement and a prolonged initial phase. These are caused by a sudden increase is the dynamic pressure of the solar wind as high speed and

high-density plasma from the Sun suddenly arrive at the Earth. The magnetopause is pushed earthward, strengthening its current and its positive effect on the ground. The sudden commencement is a packet of waves triggered by the sudden displacement of the field lines in the magnetosphere that resonate in response to the change. The initial phase lasts from a few minutes to many hours, and is usually followed by a rapid decrease in the surface field. This decrease is called the main phase of the magnetic storm. A weak storm consists of only a 50 nT decrease, a moderate storm about 150 nT, a strong storm up to 300 nT, and a great storm more than 500 nT. The main phase may last from a few hours to as many as 12 h. Eventually the magnetic field begins to recover. A typical recovery is exponential in form with a time constant of about 8 h. The recovery phase is usually over within one to 2 days.

The main phase is caused by the growth of a ring current around the Earth. This is traditionally though to be a doughnut-shaped region around the Earth containing a strong westward current. This current is primarily created by ions including protons, helium ions, and oxygen ions drifting westward around the Earth from midnight towards dusk and onward. This current acts much like a large solenoid around the Earth producing a magnetic disturbance that is southward along the Earth's dipole axis, whereas the geomagnetic field itself is northward. The recovery phase of the storm is caused by the loss of these ions. Until recently it was thought that the main loss process for the ions was charge exchange. As the ions approach the atmosphere in their bounce motion there is a high probability of interaction with an atmospheric neutral atom. An electron from the cold atmospheric atom is exchanged with the hot ion. The hot ion becomes an energetic neutral atom that is no longer confined by the field. The cold atom is transformed into a cold ion that contributes little to the current.

The creation of the ring current is caused by a prolonged interval of strong southward magnetic field and high solar wind velocity. These are precisely the conditions that cause magnetic reconnection on the dayside and intense convection in the magnetosphere. The ions creating the current are brought in from the tail and energized by the magnetospheric electric field associated with convection. There is growing evidence that most of these ions simply drift through the magnetosphere and exit through the dayside boundary (Liemohn et al., 2001). Only after the recovery phase begins do some of these ions come onto closed drift paths that circle the Earth. There is also growing evidence that ion cyclotron waves may play an important role in ring current decay. These waves scatter ions in pitch angle towards the loss cone. This allows the ions to come closer to the atmosphere where the probability of interacting with a neutral particle is higher.

There is no type of ULF wave that has been identified as specifically created by a storm-time ring current. The instabilities that can occur in a cloud of drifting protons also occur during intervals that are not strong

enough to be called storms. Every magnetic storm includes many substorms, and these are probably the cause of the ULF waves occurring during storms.

2.3 External sources of ULF waves

Many of the waves seen at the Earth's surface originate outside the magnetosphere (Yumoto, 1988). The solar wind, the foreshock, the bow shock and the magnetopause are all sources of ULF waves. Many of these waves pass through the magnetopause and propagate through the magnetosphere. Internally they interact with waveguides, cavities, and field lines creating the pulsations actually seen at the surface.

2.3.1 *Solar wind*

The solar wind is a source of ULF waves, particularly at low frequencies around 1 mHz (Belcher and Davis, 1971). Some of these waves originate at the Sun and are both carried by, and propagate through, the solar wind. A typical example of these waves is presented in Figure 8. The fluctuations in the components of the magnetic field and velocity vectors are often irregular, but with a smooth, power-law spectrum. The individual component time series of B and V are virtually indistinguishable, indicating a high correlation

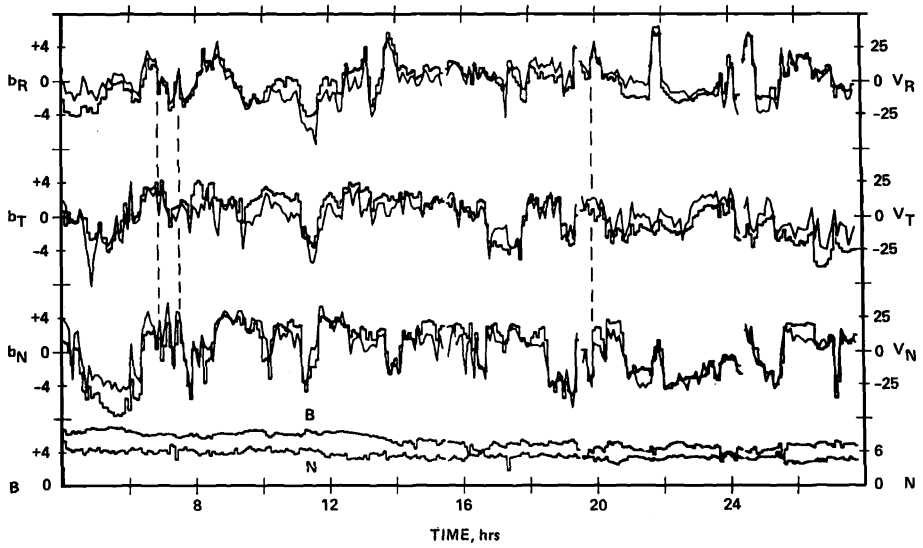

Figure 8. Alfvén waves in the solar wind magnetic field (left axis) and flow velocity (right axis). The three panels show the spherical components of the two vectors *b* and *V*. The direction (*n*) is normal to the ecliptic plane, (*t*) is azimuthal, and (*r*) is radial. The traces of B and V are virtually indistinguishable. Note the absence of variations in total field and density (Reproduced by permission of American Geophysical Union, Belcher and Davis, 1971).

between the V and B perturbations. In addition, the magnitude of B and the plasma density are virtually constant. Both observations indicate that the fluctuations are caused by Alfvén waves (the intermediate mode).

At other times there are quasiperiodic variations in the solar wind density, and hence dynamic pressure. These pressure changes cause the magnetosphere to expand and contract creating global changes in the internal magnetic field. Kepko et al. (2002) show that the spectrum of the dynamic pressure has multiple peaks at frequencies including $f = 0.4$, 0.7, 1.0, and 1.3 mHz. The simultaneous spectrum of the total field at synchronous orbit is virtually identical. The authors speculate that these waves may have originated at the Sun as pressure waves caused by granulation, and not in a magnetospheric waveguide as has sometimes been suggested (Samson et al., 1991).

2.3.2 *Ion foreshock*

The ion foreshock is another source of ULF waves seen in the magnetosphere. Figure 9 shows the relation of the ion foreshock to the bow shock

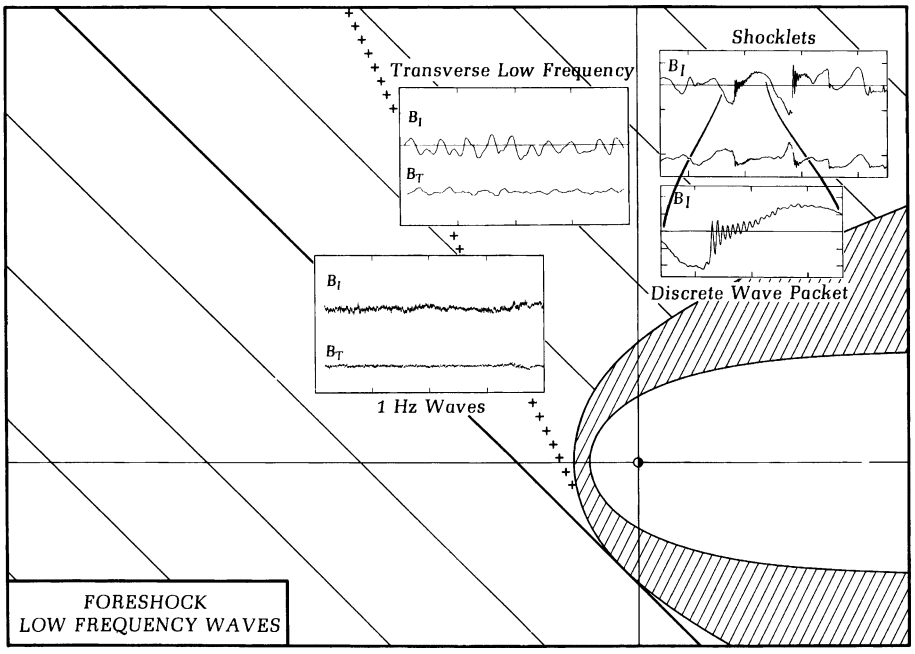

Figure 9. The electron and ion foreshocks are produced by charged particles reflected from the bow shock. As the particles move upstream along the tangent magnetic field line they interact with the solar wind producing waves. The type of waves (indicated in the three panels) depends on the distribution of particles that reach a certain point. The ion foreshock is shown here by + signs (With kind permission of Springer Science and Business Media, Russell and Hoppe, 1983).

(Russell and Hoppe, 1983). The foreshock is caused by ions moving upstream along magnetic field lines tangential to the shock. As the charged particles travel upstream they $\boldsymbol{E} \times \boldsymbol{B}$ drift in the solar wind electric field. For the geometry shown, the electric field is upward, out of the plane of the figure when the magnetic field points away from the Sun towards the Earth. Then the particle drift is orthogonal to $\boldsymbol{B}$ in the downstream direction. An oppositely directed $\boldsymbol{B}$ reverses the electric field but the drift is the same. The path followed by ions is denoted by a string of + signs. Electrons are also reflected at the bow shock and travel upstream, drifting in the solar wind electric field. The electron path is closer to the direction of the magnetic field because the heavier ions move along the field lines more slowly than the electrons.

As the ions move upstream they interact with the solar wind producing waves with frequencies that depend on the strength of the solar wind magnetic field (Russell and Fleming, 1976; Russell and Hoppe, 1983). These waves propagate very slowly relative to the speed of the solar wind so they are swept downstream towards the bow shock. The properties of the waves depend on the nature of the ion distributions (Hoppe et al., 1982; Thomsen, 1985). Close to the ion foreshock the ions are field aligned and produce small amplitude 1 Hz waves. At larger angles the distributions are more spread out around the field direction (intermediate distributions), and produce larger amplitude, lower frequency waves. At still larger angles the ion distributions become diffuse rings around the magnetic field and produce waves that steepen into miniature shocks. These three types of waves are illustrated in the inset panels of Figure 9.

The processes that produce the various ion distributions are not fully understood. In addition, the plasma instabilities that generate the waves have not all been identified. The precise nature of the ion distributions depends on the geometry of the solar wind magnetic field, and whether or not reconnection is occurring at the magnetopause.

2.3.3 *Bow shock*

The bow shock is a fast mode wave standing in the solar wind (Russell, 1985; Spreiter and Stahara, 1985). As a sharp discontinuity in space, it is made up of waves with many different frequencies. For the normal spiral orientation of the solar wind magnetic field shown in Figure 9, the field will be tangential to the shock on the afternoon side. In this region the solar wind magnetic field is orthogonal to the shock normal producing a perpendicular shock. On the morning side the shock normal and magnetic field are parallel producing a parallel shock (Greenstadt and Fredericks, 1979; Greenstadt, 1983).

The difference between the two shocks is illustrated in Figure 10. The top panel shows a quasi-perpendicular shock where the angle between the field and shock normal, Θ_{BN}, is 62°. Because the field is parallel to the shock front the waves creating the shock cannot escape and it becomes a sharp discon-

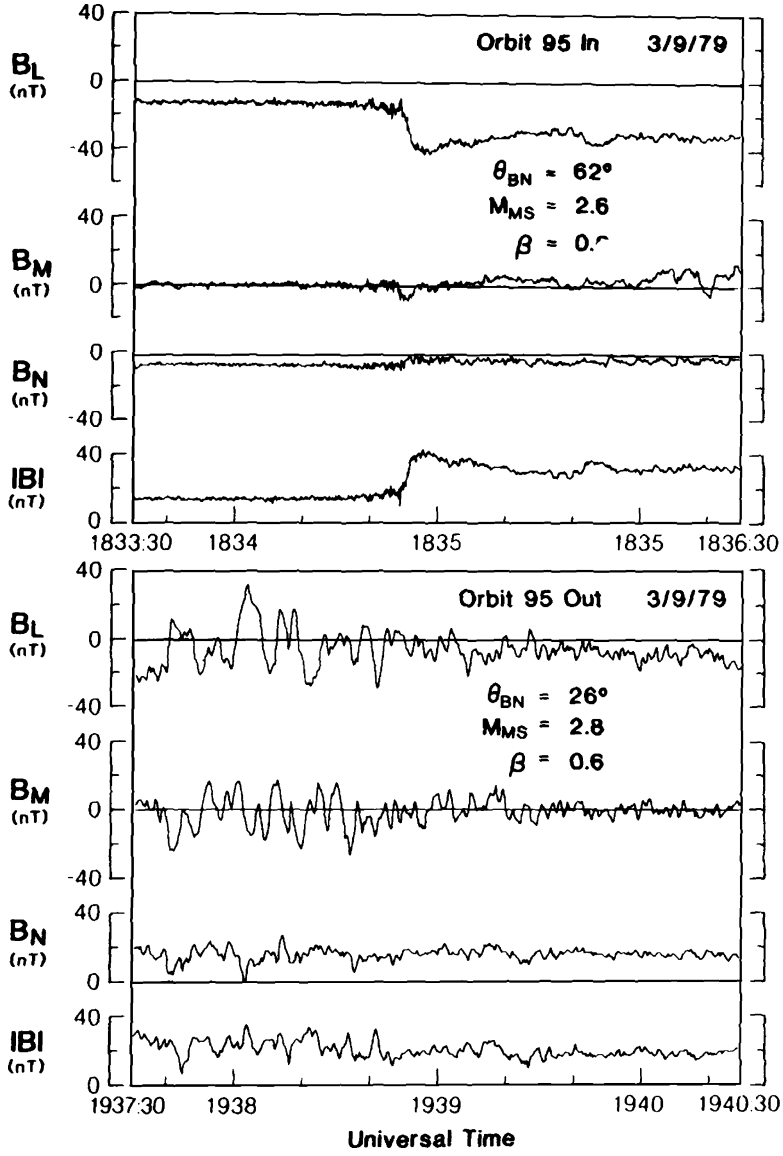

Figure 10. Different components of the magnetic field variations observed at the Earth's bow shock. The top panel shows a quasi-perpendicular shock ($\Theta_{BN} = 62°$) (see text), and the bottom panel shows a parallel shock ($\Theta_{BN} = 26°$). Both the solar wind magnetosonic (MS) Mach number, the ratio of the solar wind velocity to the magnetosonic velocity, and plasma beta, the ratio of the magnetic pressure to the thermal plasma pressure, are the same (Reproduced by permission of American Geophysical Union, Russell, 1985).

tinuity. The bottom panel shows a quasi-parallel shock ($\Theta_{BN} = 26°$). In this case the waves escape from the shock front along field lines producing a highly turbulent transition. The parallel shock is a source of ULF waves that propagate downstream and, under certain circumstances, can enter the magnetosphere.

The penetration of solar wind waves, upstream waves and bow shock waves into the magnetosphere depends on the cone angle of the solar wind magnetic field relative to the Earth–Sun line. The most common situation is a magnetic field oriented at the spiral angle as shown in Figure 9 where the cone angle is 45°. Then the upstream waves and the parallel shock are located on the dawn side of the Earth. Waves from this region will be swept downstream through the shock and into the magnetosheath, generally following streamlines (as illustrated in Figure 11). In the case shown the waves will miss the magnetopause. However, if the solar wind magnetic field rotates to a radial direction, then upstream waves, and the parallel shock will be located immediately in front of the Earth and the stagnation field line will

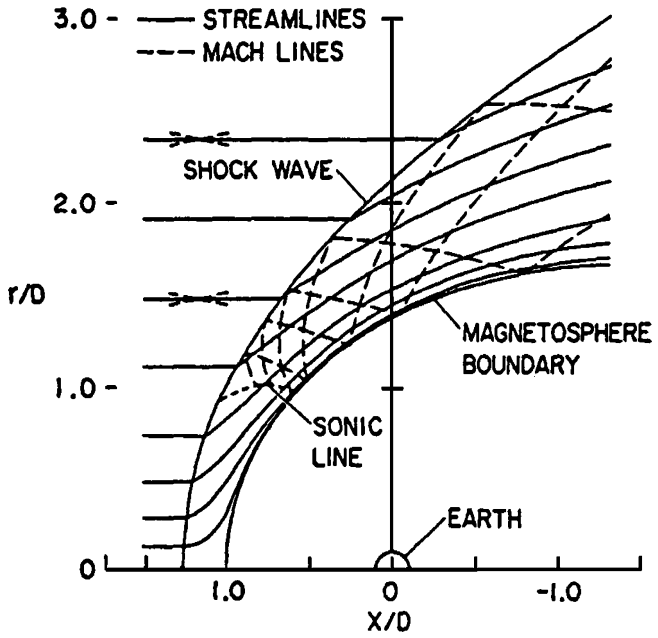

Figure 11. Streamlines in the solar wind at the left pass through the bow shock into the magnetosheath. Only streamlines close to the subsolar point of the bow shock (bottom left) come close to the magnetopause. Disturbances on streamlines near the top of the diagram pass around the Earth far from the magnetopause (Spreiter and Stahara, 1985). The radius of the subsolar magnetosphere, D, is generally near 10 Earth radii (10 Re) (Reproduced by permission of American Geophysical Union).

contain many fluctuations that impact the magnetopause and enter the magnetosphere (Greenstadt et al., 1979b; Takahashi et al., 1981).

2.3.4 *Magnetopause*

The magnetopause is a source of several types of ULF waves. One type is produced by oscillatory dynamic pressure fluctuations in the solar wind as discussed above (Kepko et al., 2002). As the pressure increases the magnetopause current strengthens and moves closer to the Earth globally increasing the magnetic field inside. As the pressure decreases the current moves out and weakens, reducing the internal field.

Another type of wave is caused by step like changes in the dynamic pressure (Southwood and Kivelson, 1990). For example, a sudden pressure change will cause a ring-shaped distortion around the magnetopause that moves downstream with the flow. Behind the step the magnetopause has a different diameter than it does ahead of the step. The boundary perturbation will be "S-shaped" when projected in the equatorial plane. The vorticity produced by this step generates a pair of oppositely directed field-aligned currents connected to the magnetosphere as illustrated in Figure 12. The

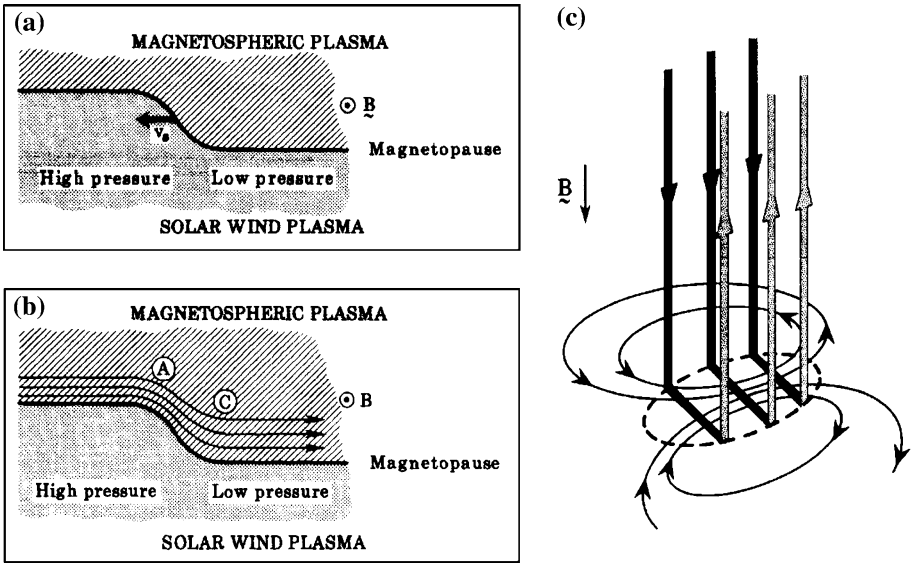

Figure 12. Generation of a pair of FAC by a step-like change in the diameter of the magnetopause due to a decrease in dynamic pressure. (a) shows the step propagating to the left in the rest frame of the magnetosphere. (b) shows the apparent flow in the rest frame of the step. The streamlines indicate a vortical flow with FAC out of the equator at A and into the equator at C. In (c) these FAC close in the ionosphere through a Pedersen current (horizontal bars), and also generate a Hall current (thin lines) (Reproduced by permission of American Geophysical Union, Southwood and Kivelson, 1990).

FACs close in the ionosphere through a Pedersen current that shields the ground from the effects of the FACs (Fukushima, 1969). A solenoidal Hall current is also generated and circulates in the ionosphere around the pair of currents, creating a vortex of current flow. The magnetic effects of this Hall current are seen on the ground as a magnetic impulse that moves across a station array. An example of data from a high latitude chain of magnetometers on the west coast of Greenland at local noon (Ridley et al., 1998) is presented in Figure 13. The three panels show the X, Y, and Z components of the perturbation field with the northernmost station at the top of the panels. A sequence of pulses with amplitude exceeding 100 nT is evident in all components.

The cause of these disturbances is more evident when the data are plotted as equivalent ionospheric convection as is done in Figure 14. At each time point the horizontal field perturbation vectors are rotated 90° counter clockwise (CCW) and plotted along a time line scaled so that the direction of the vector indicates the North and East components of the ionospheric flow. In the diagram time is plotted from right to left, and latitude from bottom to

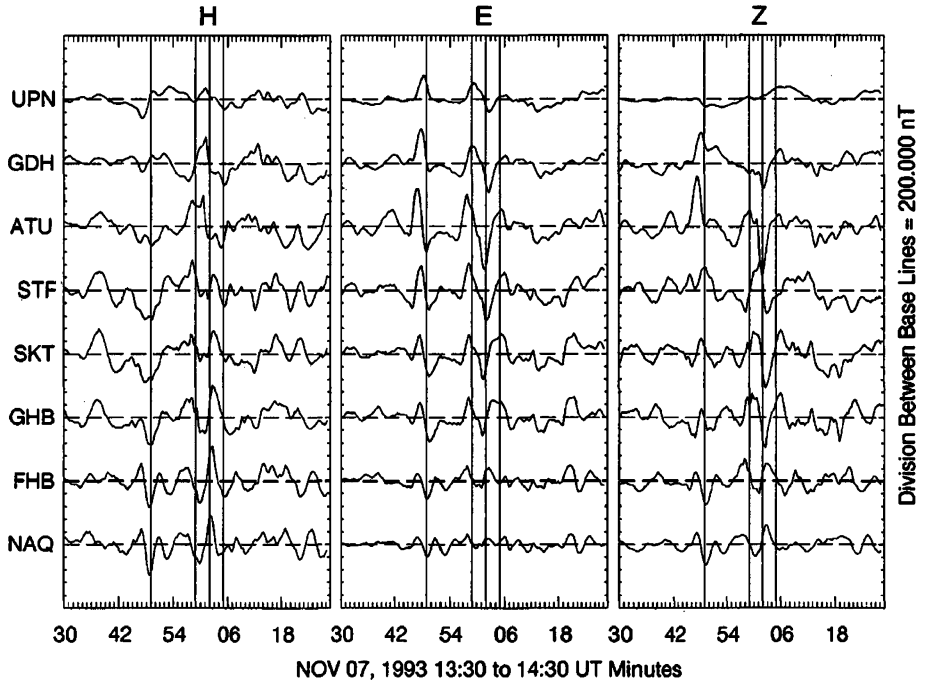

Figure 13. The North (H), East (E) and downward (Z) components of the magnetic field recorded by a latitude chain of magnetometers (North at top) on the West coast of Greenland observed during a sequence of TCVs (Reproduced by permission of American Geophysical Union, Ridley et al., 1998).

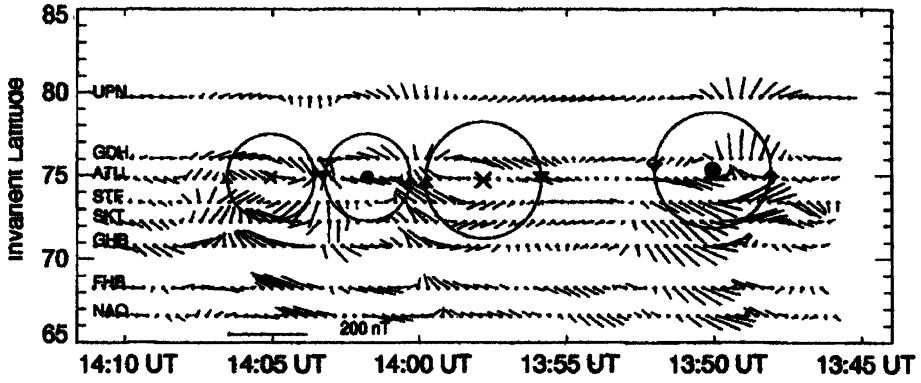

Figure 14. An equivalent ionospheric flow diagram obtained from Error! Reference source not found. by rotating the horizontal magnetic perturbation vectors at each station 90° counterclockwise. Time runs from right to left and latitude increases towards the top of the diagram. Circles denote the direction of ionospheric flow around the centers of successive vortices. Dots and X's denote FACs out of, and into, the ionosphere (Reproduced by permission of American Geophysical Union, Ridley et al., 1998).

top. Since Eeast–West time delays show that the disturbances are moving eastward, successive vertical lines show the perturbation profiles that will move across the array as time increases. For example, the disturbance centered on 13:50 UT is a counter clockwise convection vortex produced by an outward field-aligned current. The Hall current causing the ground perturbations is everywhere opposite to the direction of convection. Altogether, four vortices formed and crossed the array in the time interval shown in the figure. Ridley et al. (1998) use data from other stations to show that the vortices do not usually live long enough for more than one to be present at a time. They show that these vortices were born at about 10 local time, propagated eastward across the chain located at noon, and died to the East of the chain in early afternoon.

Although the ionospheric form of the vortices shown in Figure 14 is identical to those expected from the mechanism described by Southwood and Kivelson (1990) other data suggest that a different process caused this event. The authors note that there were no pressure fluctuations in the solar wind, but that the solar wind magnetic field was southward and reconnecting to the Earth's field at the subsolar point. In addition, during the event the By (dawn-dusk) component of the solar wind was oscillating, causing ionospheric flows near noon to change direction. They speculate that these vortices were caused by a change in the FAC associated with these oscillations in By. Other authors have suggested additional causes of traveling convection vortices (TCVs). For example, McHenry et al. (1990) provided evidence that many vortices are created inside the magnetopause near the inner edge of the low latitude boundary layer. During strong convection this interface is the

site of a large shear in the plasma velocity between field lines moving tailward in the boundary layer and other field lines returning to the dayside; hence it may be unstable to the Kelvin–Helmholtz instability. Yahnin and Moretto (1996) have used low-altitude satellite charged particle measurements to take issue with the earlier work and argue that " ...TCVs map to regions inside the plasma sheet which are well separated from the LLBL/Mantle region by BPS type precipitation".[2] Thus, they suggest that it is unlikely that any of the three mechanisms previously postulated (pressure pulses, Kelvin–Helmholtz instability, and reconnection) can account for the observations. Regardless of the eventual outcome of this controversy, traveling convection vortices are a continual source of magnetic disturbance at very high latitudes ($\sim$75° magnetic).

3. Transmission of ULF waves through the magnetopause

Waves created outside the magnetosphere must pass through the magnetopause to be seen at the ground. How well they can do this is not known. Attempts have been made to measure the transfer function of the magnetopause for ULF waves, but with little success (Greenstadt et al., 1983; Engebretson et al., 1987, 1991; Lin, 1991). The main problem is getting two spacecraft on opposite sides of the boundary near the same meridian for a sufficient length of time to determine the transfer function. Despite these difficulties, it is clear that considerable ULF wave energy does enter the magnetosphere. Figure 15 demonstrates that the probability of observing Pc 3 pulsations at synchronous orbit (6.6 Earth radii) depends on the solar wind conditions (Takahashi et al., 1981). Synchronous Pc 3 pulsations occur with very high probability when the solar wind velocity is high and the solar wind magnetic field is radial. A number of studies show that the amplitude of Pc 3 pulsations on the ground depends on these same parameters (Singer et al., 1977; Greenstadt et al., 1979a, b).

The ULF waves seen at the ground are not usually the same wave that enters the magnetosphere from the solar wind. The wave energy is transformed and amplified by processes inside the magnetosphere as discussed in the following section.

3.1 Internal amplification of ULF waves

Two processes transform the ULF wave energy that enters the magnetosphere from outside. One is called field line resonance and the other cavity

[2] Low Latitude Boundary Layer (LLBL), Boundary Plasma Sheet (BPS)

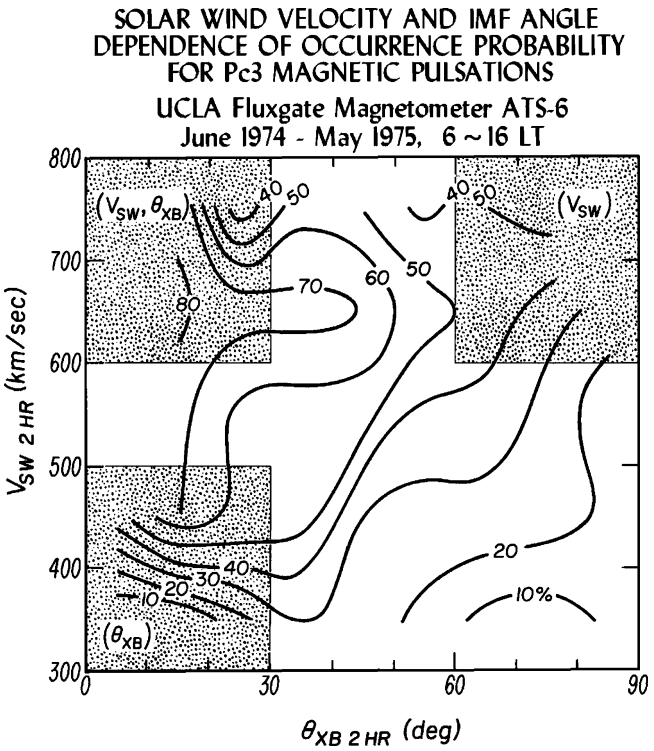

Figure 15. The probability of observing Pc 3 magnetic pulsations at synchronous orbit is shown as a function of the velocity of the solar wind (V_{sw}) and the angle between the Earth–Sun line (*x*-axis) and the direction of the field (θ_{XB}). Note the very high probability when the velocity is high and the field is radial (Reproduced by permission of American Geophysical Union, Takahashi et al., 1981).

resonance. Magnetic field lines behave like stretched strings (Southwood and Hughes, 1983). The cavities between various boundaries act like resonant cavities or waveguides (Kivelson et al., 1984). The two processes interact with each other. Standing waves in the cavities feed energy to the field line resonances. Many of the pulsations seen at the ground are radiated from the ends of field lines set into motion by a complex process involving coupling of the propagating waves to resonant cavities, and these in turn coupling to field line resonances.

3.1.1 *Field line resonances*

Field lines of the Earth's dipole behave like vibrating strings as illustrated in Figure 16. The ends of the field lines are frozen in the conducting ionosphere and cannot move, although they can bend. In their equilibrium positions there is no force orthogonal to the field lines. However, if some process displaces a field line, a tension force develops that tries to restore it to its

equilibrium shape. However, because the field line is loaded with gyrating particles it picks up momentum that causes it to overshoot the equilibrium. The field line thus oscillates until other processes cause damping.

There are two primary modes of oscillation of a dipole field line (Southwood and Hughes, 1983). The toroidal mode is a displacement in the azimuthal direction creating an azimuthal magnetic perturbation, as shown in the right panels of Figure 16. The poloidal mode is a radial displacement with radial magnetic perturbations as shown in the middle panels. Either mode may oscillate with different harmonics. The fundamental harmonic depicted in the top row contains an odd number (one) of half wavelengths between the ends of a field line. The second harmonic in the bottom row contains an even number (2) of half wavelengths. Many different harmonics may be simultaneously excited when the field line is excited by a broadband source.

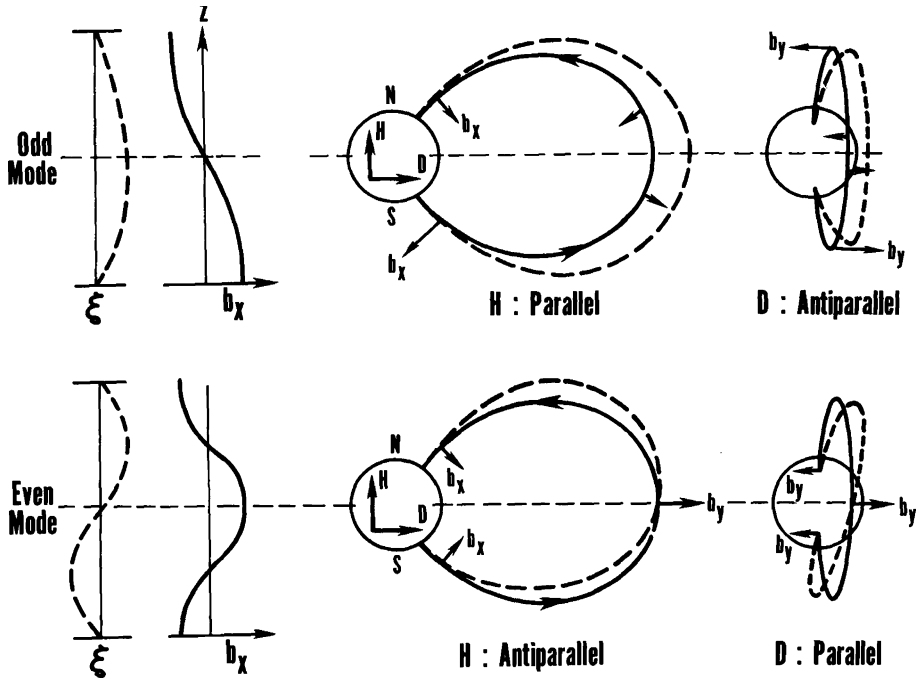

Figure 16. The field lines of a dipole (middle panels) may be approximated as stretched strings (left panels). The dipole lines may be displaced and oscillate in two orthogonal directions – radial (center panels) and azimuthal (right panels). The oscillation may consist of odd (top row) or even (bottom row) harmonics. The field lines are anchored at the ends (ionosphere) and are nodes of field line displacement, but antinodes of the magnetic perturbation. In the diagram ξ denotes the field line displacement and b_x and b_y are the components of the magnetic perturbation (Modified by permission of American Geophysical Union, Sugiura and Wilson, 1964).

The toroidal mode of field line resonances is most commonly observed in space. The reason is that azimuthal perturbations do not change the field magnitude or cause plasma density changes. In addition, field lines azimuthally adjacent to the vibrating line have nearly the same resonant frequency and so can vibrate in phase with the initially disturbed line. In fact, these properties identify this mode as the Alfvén wave. The poloidal mode is harder to excite because field lines are oscillating in a radial direction and radially adjacent field lines have different frequencies. Inevitably, adjacent field lines will oscillate out of phase and there will be compressions and rarefactions of the field. This mode of field line resonance corresponds to the fast mode.

The simplest approximation to the fundamental frequency of a field line is obtained by integrating the Alfvén travel delay $dt = ds/V_A$ along a field line. The local delay depends on both the field strength and the plasma density through V_A. Longer field lines have longer resonant periods (lower frequencies). Field lines with more, or heavier, particles will also have longer periods. This behavior of the Alfvén velocity and resonant frequency is shown in Figure 17 taken from Waters et al. (2000). In the simple model used to obtain these curves, the magnetopause is located at 10 Re, the plasmapause at 5 Re, and the ionosphere at 1.1 Re. The sudden decrease in velocity and frequency at about 5 Re is caused by the increase in plasma density going inward across the plasmapause. The decrease close to the ionosphere is caused by the presence of oxygen ions in the upper ionosphere. The slow increase in resonant frequency from 3 mHz at the magnetopause to 20 mHz

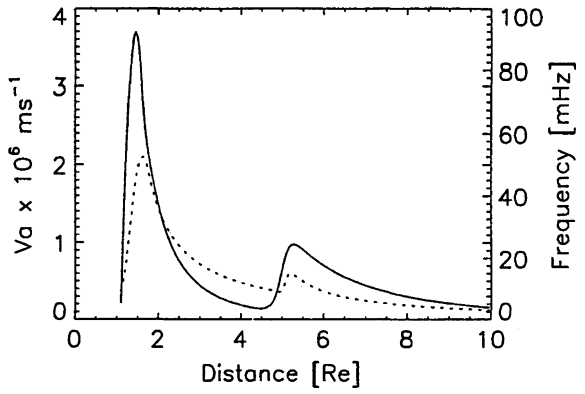

Figure 17. The radial profile of Alfvén velocity (solid line) and field line resonance frequency (dashed line) in the magnetosphere. In this model the magnetopause is located at 10 Re, the plasmapause at 5 Re, and the ionosphere at about 1.1 Re. Note that the increase in density at the plasmapause causes the Alfvén velocity and resonant frequency to decrease sharply. The decrease near the ionosphere is caused by a rapid increase in the density of oxygen ions (Reproduced by permission of American Geophysical Union, Waters et al., 2000).

at the plasmapause, and a much larger increase inside the plasmapause, are caused mainly by a rapid increase in field strength and a decrease in field line length. Although the plasma density increases inward, this change is too slow to overcome the effects of the magnetic field.

Any process that displaces a field line can excite field line resonances. The most common source is ULF waves propagating through the magnetosphere after having been transmitted through the magnetopause. Another source is waves created at the magnetopause that are evanescent inside the magnetosphere (spatially damped). A third source is sudden changes in magnetospheric plasma flow velocity such as those that occur in substorms. Another source is internal plasma instabilities as discussed below.

3.1.2 *Latitude profiles of the amplitude and phase of resonant pulsations*
Because the most common source of ULF wave energy on the ground is field line resonances, it is important to understand the structure of a resonance in space, and how the ionosphere alters this structure. The amplitude and phase of the electric field of a resonant auroral zone field line measured by radar in

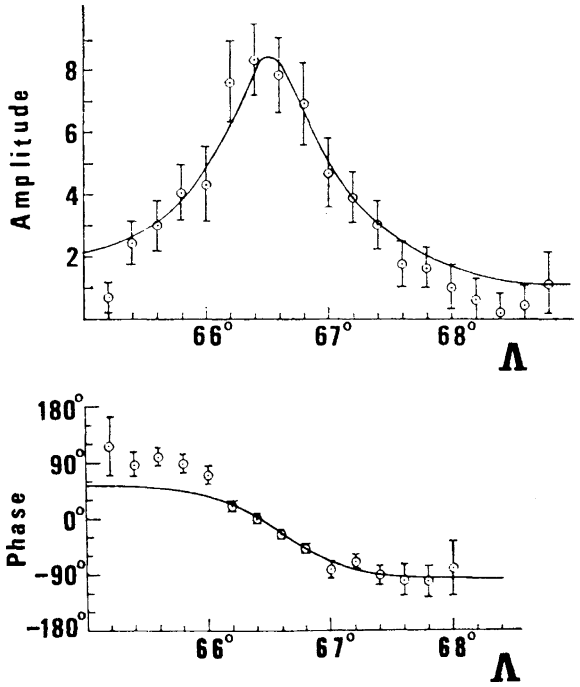

Figure 18. Properties of the electric field of a resonant field line in the auroral zone as measured by radar (Walker and Greenwald, 1980). The top panel shows the signal amplitude as a function of latitude (Λ); the bottom panel shows the phase. The solid lines are the values expected at the ground from theory.

the auroral zone is displayed in Figure 18 (Walker and Greenwald, 1980). The amplitude shows the expected structure of a resonance, with a peak amplitude at a fixed latitude (Southwood, 1974). The phase profile is also typical of a resonance, lagging the resonant signal on one side and leading on the other. Ideally the phase changes by 180° across a resonance. In this example the half width for this change is less than a degree, or about 100 km. Clearly, the phase of this wave on the ground changes rapidly in the North–South direction.

In the example shown in Figure 18, only one shell of field lines was excited; hence, only one frequency was observed on the ground. More typically, the spectrum of the source that excites the resonant shell of field lines is broadband and multiple harmonics are generated on a single shell (Takahashi and McPherron, 1982). In addition, adjacent shells will also be excited and exhibit the same type of resonant behavior, but peaked at slightly different latitudes. The result on the ground is a complex, broadband spectrum in which it is nearly impossible to detect resonant peaks in amplitude or phase reversals unless one uses special techniques (Chi and Russell, 2001).

3.1.3 *Effects of the ionosphere*

The ionosphere has a variety of effects on the waves seen at the ground (Hughes, 1974). First, it should be understood that the signal seen at the ground is an electromagnetic wave radiated from currents induced in the ionosphere, and not the hydromagnetic wave that was incident. Second, the ionosphere can have a strong effect on the polarization of the wave. For example, an incident toroidal mode will have its magnetic polarization in the East-West direction. As shown schematically in Figure 19, the FAC driven by the Alfvén wave will close both North and South of the resonant shell via Pedersen currents. These currents produce ground perturbations that nearly cancel the ground perturbations of the FAC (Fukushima, 1969). The $\boldsymbol{J} \times \boldsymbol{B}$ force from the Pedersen closure drives a vortical flow in the ionosphere. Because the ions suffer more collisions than the electrons, there is a Hall current in the opposite direction (shown by dashed lines). Magnetic effects of the Hall current are seen on the ground as a magnetic perturbation that has been rotated 90° CCW relative to the field of the incident wave. Thus, toroidal modes in the magnetosphere will have N–S polarization on the ground. If the width of the resonance is less than the height of the ionosphere (100 km) the signal on the ground will be significantly attenuated by spatial filtering effects (Hughes, 1983). Also, if the size of the ULF wave source in the ionosphere is limited there will be strong vertical components observed on the ground (Southwood and Hughes, 1978).

A third effect of the ionosphere is a consequence of a resonant cavity. The rapid increase in molecular weight from the top of the ionosphere down causes a reduction in Alfvén velocity from magnetospheric values. Then, at

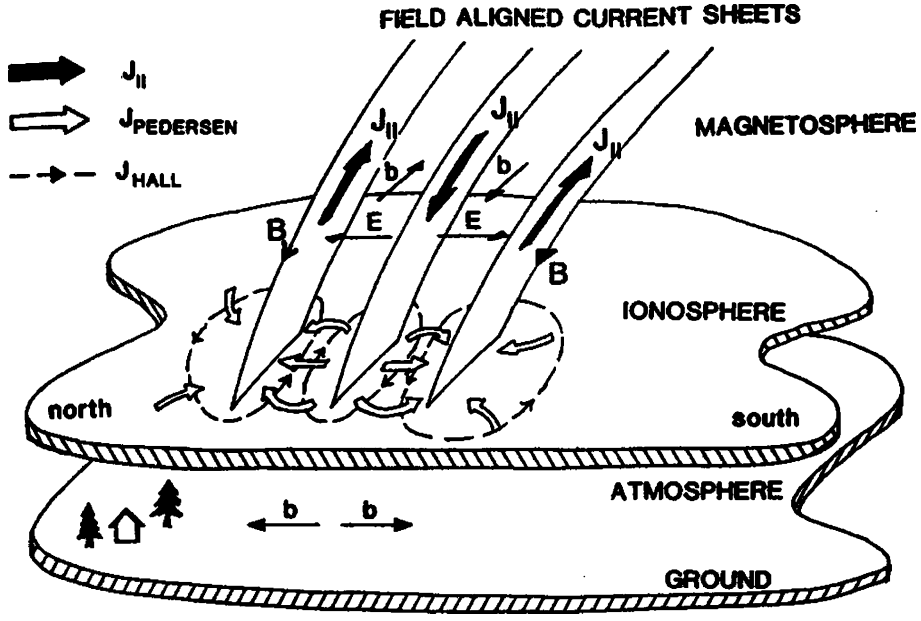

Figure 19. The ionospheric currents driven by a toroidal resonance. The incident wave is an Alfvén wave with East–West polarization and FAC. The FAC close N–S via Pedersen currents. These currents cancel the magnetic effects of the FAC. A Hall current created by the $\mathbf{J} \times \mathbf{B}$ forces of the wave produces the magnetic field seen at the surface that is rotated 90° CCW (With kind permission of Springer Science and Business Media, Hughes, 1983).

the bottom of the ionosphere the rapid decrease in electron and ion density causes an increase in Alfvén velocity up to the speed of light. Together these effects create a low velocity layer with thickness of order 100 km that resonates to waves with frequency near 1.0 Hz (Lysak, 1988). This region of the ionosphere is known as the ionospheric waveguide; it plays a major role in the ducting of Pc 1 pulsations from high to low latitudes. It should be noted that, since the Pc 1 waves are propagating towards the equator from the auroral zone, the Earth's surface is not a surface of constant phase.

3.1.4 *Cavity resonances*

We mentioned above that the boundaries within the magnetosphere form cavities that may also resonate in response to external excitation. If we approximate the magnetosphere as a spherical cavity then it is obvious that the region between the magnetopause and the plasmapause forms a complex, doughnut-shaped cavity. We might expect this cavity to have normal modes with standing waves both radially and azimuthally, as well as along the field lines. However, because of the tail the magnetosphere is more like a waveguide than a cavity. Waves can "stand" radially, but will propagate azimuthally and be lost down the tail.

Numerous authors have studied this problem and obtained analytic solutions for various simplified geometries (Radoski, 1971; Kivelson et al., 1984; Allan et al., 1991; Samson et al., 1992; Rankin et al., 1995; Walker, 1998). Others have used numerical methods to simulate magnetospheres that are more realistic (Lee and Lysak, 1989, 1991; Samson et al., 1991, 1995; Ding et al., 1995; Mann et al., 1995; Rickard and Wright, 1995; Waters et al., 2000; Keller and Lysak, 2001). The real magnetosphere is extremely complex because of the asymmetric magnetic field with strong gradients in field and plasma in every direction. In addition, its dimensions are continually changing in response to the solar wind so the cavity properties are always changing. These facts have made it difficult to demonstrate conclusively the existence of cavity modes experimentally (Radoski, 1971; Crowley et al., 1987; Samson et al., 1991; Kivelson et al., 1997). There is, however, some

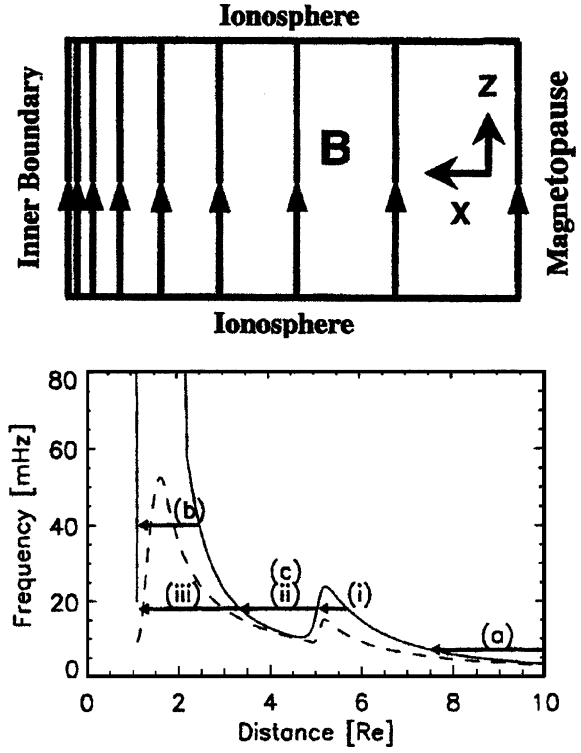

Figure 20. A 1-D model of the magnetospheric cavity near local noon. The ionosphere is at the left and the magnetopause at the right. The top panel indicates that the field lines have been straightened placing the northern and southern ionospheres at the top and bottom of the box and that the field strength decreases outward. The bottom panel shows the field line resonant frequency (dashed line) and the turning points of the differential equation as a function of radial distance. Regions (a)–(c) are discussed in text (Reproduced by permission of American Geophysical Union, Waters et al., 2000).

indirect evidence discussed next that they exist and are an important factor in determining the properties of ground ULF waves.

To illustrate the nature of cavity resonances we review a recent paper by Waters et al. (2000) who solved a 1-D cavity model of the magnetosphere. The two diagrams in Figure 20 summarize the model. In the top panel, dipole field lines are straightened and fixed in conducting ionospheres at the top and bottom of the box. The strength of the field decreases as the inverse cube of distance from the ionosphere on the left to the magnetopause on the right. In addition, the plasma density varies with distance to simulate the natural radial variation. From the magnetopause inward, the density gradually increases until the plasmapause where it steps up by a factor of about 100. The density then again gradually increases to the top of the ionosphere where the average mass begins to increase rapidly as the plasma density falls. Finally at the bottom of the ionosphere the charge density vanishes allowing the velocity to increase to that of electromagnetic waves in a neutral gas. These assumptions produce the Alfvén velocity profile shown by a solid line in Figure 17. Dashed curves in Figure 17 and the bottom panel of Figure 20 denote the field line resonance frequency associated with this profile. There are two cavities in the radial direction. Waves can stand radially between the magnetopause and the plasmapause, and between the inner side of the plasmapause and the ionosphere.

In this 1-D box model it is assumed that waves will stand both along field lines and radially, but propagate azimuthally. To more closely simulate the circular structure of the Earth's field the azimuthal wavelength of the propagating wave was chosen to increase proportionally to radial distance, i.e. from left to right. The model assumes that cavity modes couple energy into the field line resonances, and that the field line resonances are damped by the conductivity of the ionosphere. The inner boundary at the ionosphere is taken to be a rigid boundary that does not allow radial displacement of field lines. However, to drive the system, the outer boundary at the magnetopause is displaced radially with a spectrum inversely proportional to frequency.

The radial displacement of the boundary by an azimuthally propagating wave produces a disturbance inside the magnetosphere that stands in the radial direction while propagating in the azimuthal direction. Since the cavity is open in the azimuthal direction, these waves are better called waveguide modes. At a radial distance called the turning point, the waves cease standing in the radial direction and become exponentially damped. The turning point is effectively the inner boundary of the radially standing wave, although there is evanescent penetration inside the turning point. The radial location of the turning point for any frequency is shown by the solid line in the bottom panel of Figure 20. For a given frequency, the turning point is always radially outside the location of a field line resonance of the same frequency. This can

be seen by drawing a horizontal line from the resonant frequency (dashed line) to the turning point (solid line). Thus, the only way to couple a radially standing wave to the field line resonance is through its evanescent tail.

Since the waves must stand in the radial direction there are only discrete frequencies at which this is possible. Although the input spectrum is continuous, the radial magnetic perturbation inside the magnetosphere grows to a significant amplitude only at the discrete frequencies of the harmonics of the radially standing waves. Each harmonic of the cavity mode then couples to a field line resonance of the same frequency somewhere in its evanescent tail. At the coupling point the azimuthal component of the magnetic perturbation will grow to a large amplitude because energy from the cavity mode is fed into the field line resonance. At high latitudes the model indicates that this field line resonance may have an amplitude 10 times as large as that of the cavity mode. Because of the complex Alfvén velocity profile, the harmonics do not fit a simple pattern of integer multiples of some fundamental frequency. The lowest frequency mode is about 6 mHz, with higher harmonics separated by about 3–4 mHz. The ground spectrum produced by the coupling of cavity modes to field line resonances is very complex with many closely spaced peaks.

There are four types of cavity modes possible in this model. The first labeled (a) is bounded by the magnetopause and a turning point in the plasma trough. In the diagram this mode is denoted by the heavy line beginning at the magnetopause and ending with an arrowhead at its turning point. This mode produces field line resonances at high latitudes beyond the plasmapause. A second mode labeled (b) in Figure 20 has two turning points deep inside the plasmasphere. A single line is drawn between the two turning points with the arrowhead denoting the innermost one. The radial dependence of the amplitude and of phase of this mode are shown in Figure 21. The top panel shows that this high harmonic has 12 nodes in the radial direction. Across each node the phase of the wave changes sign. This mode couples to field line resonances very close to the ionosphere at distances of about 1.38 and 2 Re, but the inner resonance is too weak to identify. Everywhere except at the field line resonance the azimuthal component (bby) is quite weak, as seen in the bottom panel.

The behavior of the cavity modes is made more complicated by the peaks in field line resonance frequency and turning point frequency caused by the plasmapause. In Figure 20, waves of certain frequencies may tunnel through the plasmapause and stand in the internal cavity which it creates. Such waves have been called tunneling modes when one turning point is in the plasma trough and the second turning point is well inside the plasmapause. If, instead, the outer turning point is close to the plasmapause and the inner one is well inside they have been called trapped plasmapause modes. In the model discussed here these modes were not distinct and have been labeled (c). They

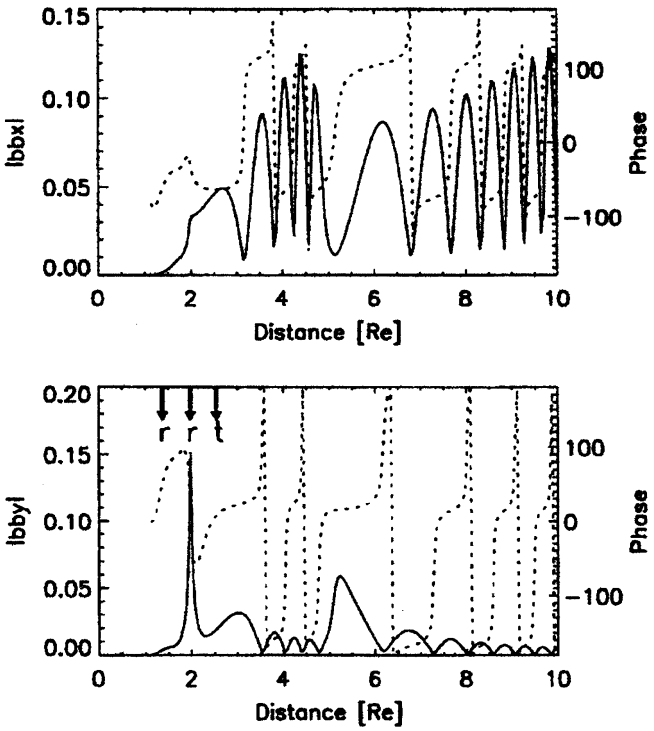

Figure 21. The radial (x) and azimuthal magnetic field perturbations (y) of a 36.8 mHz cavity resonance. The solid line shows the radial profile of the amplitude, and the dashed line shows the phase. Resonances (r) and turning points (t) are shown by arrows. This mode couples to a field line resonance at very low latitudes (distance ~2Re) (Reproduced by permission of American Geophysical Union, Waters et al., 2000).

are characterized by having two turning points close to the plasmapause and one deep inside the plasmapause. Another factor contributing to the complexity of the ground spectrum is the coupling of cavity modes to higher harmonics of field line resonances. In addition, a structured input spectrum may preferentially excite certain harmonics of the cavity mode and hence the corresponding field line resonances.

A recent paper by Waters et al. (2002) attempts to find spacecraft evidence that cavity resonances are the energy source for field line resonances observed on the ground. Despite sophisticated tests that work with MHD simulations of these resonances, all satellite data analyzed to date fail to confirm this process. The authors suggest that it is still possible that impulsive sources of fast mode waves propagating through the cavities might couple to field line resonances. Unfortunately, there is no evidence that a source with sufficient frequency and amplitude of impulses exists.

4. Internal sources of ULF waves

To this point we have only considered ULF waves generated externally to the magnetosphere and how they are affected by the magnetosphere and ionosphere. A variety of internal plasma instabilities can also generate ULF waves. The frequencies of these waves tend to be controlled by properties of the charged particle distributions that provide the energy, but they are also affected by the Alfvén velocity profiles. In general there are three periodicities associated with charged particles trapped in the dipole geomagnetic field; gyro frequency, bounce frequency, and longitudinal drift frequency. These depend on the energy and equatorial pitch angle of the particles. Corresponding to these frequencies are the cyclotron instability, the bounce resonance instability, and the drift instability. Pc 1 waves are created by the ion cyclotron instability. Some Pc 4 waves are created by a bounce resonance. Pc 5 waves can be created by a drift resonance.

Other processes also produce ULF waves. For example, bursty Earthward flows are often seen in the plasma sheet on the nightside of the Earth during geomagnetic activity. These flows radiate Alfvén waves that travel to the auroral ionosphere where they are reflected and travel back to interact with the flow. This process is though to create Pi 2 waves. High frequency components of these waves (Pi 1) seen on the ground may be produced in a resonant cavity between the topside of the ionosphere and the auroral acceleration region at $\sim$1 Re altitude that is excited by fluctuating FACs (Pilipenko et al., 2002). In the following, we briefly describe several of the most common processes and illustrate how ULF waves are generated internally in the magnetosphere.

4.1 Gyro resonance

Gyro resonance (or cyclotron resonance) applies to the situation where a circularly polarized wave and a charged particle rotate (gyrate) about the magnetic field at the same frequency. Because the electric field of the wave and the particle velocity maintain a constant angle with respect to each other, the field is able to exert a force on the charge for a long interval. This allows energy transfer to occur (Brice, 1964). In which direction the energy flows depends on the relative angle. In the magnetosphere cyclotron resonance between a left circularly polarized wave and protons is the mechanism that creates Pc 1 magnetic pulsations (0.5–5 Hz). This physical process is briefly described in the following paragraphs.

At frequencies close to the ion gyrofrequency, the positive ions present in a plasma significantly affect the phase velocity of an Alfvén wave. The wave becomes left circularly polarized and its velocity decreases to zero as the wave frequency approaches the ion gyrofrequency. Above the gyrofrequency, this

wave does not propagate. Suppose that a wave with frequency ω is traveling along a magnetic field line $\boldsymbol{B}$ with phase velocity V_A from the equator towards the northern hemisphere as illustrated in Figure 22. Next suppose that a proton is traveling in the opposite direction towards the equator with a parallel velocity $V_{||}$. In the reference frame of the proton, the source of the wave will appear to be approaching so that the wave frequency will be Doppler shifted to a higher frequency ω'

$$\omega' = \left(1 + V_{||}/V_A\right)\omega$$

Provided that the ion has a finite perpendicular velocity $V_\perp$, it will be gyrating about the field in a left-handed sense with the ion gyrofrequency Ω_i. When the Doppler shifted wave frequency is the same as the ion gyrofrequency the electric field and ion velocity will be in resonance. If the wave electric field is antiparallel to the ion velocity the particle will be slowed down and the wave will gain energy. In the process the pitch angle of the ion (the angle between the velocity vector and the magnetic field) must decrease to conserve total energy.

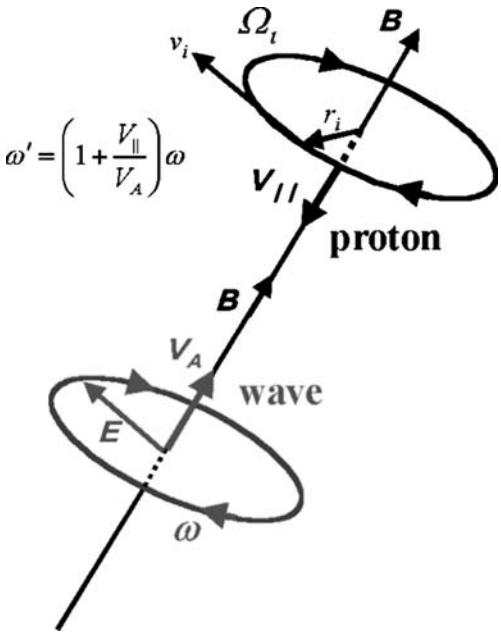

Figure 22. The ion cyclotron resonance occurs when a left circularly polarized Alfvén wave appears to a moving ion to have a Doppler shifted frequency equal to its gyrofrequency. For these conditions the particle and wave can interchange energy, either amplifying or damping the wave depending on the angle between velocity and electric field.

The wave is equally likely to lose energy as gain energy when the ions are not bunched in phase. It would seem, therefore, that the net effect would be no change in wave energy. However, if the pitch angle distribution of the ions is peaked at large pitch angles, i.e. they have more perpendicular energy than parallel energy, then on the average the wave gains energy from the ions (Cornwall, 1965). The reason for this is diffusion in pitch angle. Each interaction that damps the wave must increase the pitch angle of an ion, while interactions that grow the wave decrease the pitch angle. Pitch angle distributions in the magnetosphere are usually peaked at 90° so that there are more ions that can move to smaller pitch angles thus energizing the wave, than there are ions of low pitch angle that can move to large pitch angles.

Two processes in the magnetosphere create the necessary pitch angle distributions. The first is particle precipitation to the atmosphere. Any particle whose pitch angle becomes too small will collide with atmospheric particles and so will be lost before being mirrored. Thus, there is always a hole in the pitch angle distribution near zero degrees. This hole (loss cone) helps to maintain the gradient responsible for both pitch angle diffusion and wave growth.

The second process is magnetospheric convection discussed in the Introduction. Particles generally enter the magnetosphere in the tail and are transported Sunward as part of a two-celled convection pattern. As the charged particles approach the Earth, they begin to gradient and curvature drift across the electric field created by the convection. This drift moves them in the direction of the convection electric field so that they gain perpendicular energy. They also gain parallel energy due to the shortening of field lines, but not as rapidly, so the pitch angle distribution becomes peaked at 90°.

There are two main type of Pc 1 seen on the ground near the auroral zone. These are called Pearl Pulsations (PP) and IPDP. Both are created by the ion cyclotron instability but under different circumstances. It has long been thought that PPs are created by a wave packet bouncing back and forth between opposite ionospheres. Each time the wave packet passes through the equatorial region it interacts with protons stimulating them to emit waves of the same frequency that amplify the initial signal. The process depends on good reflection at the ionosphere, and a proton distribution with the right energy and pitch angle distribution. The Alfvén wave is dispersive near the gyro frequency, with high frequencies traveling slower than low frequencies. Because of this the wave packet becomes dispersed. Dynamic spectra of these pulsations typically exhibit a sequence of rising tones that repeat with the bounce frequency of the wave, and whose slopes decrease with time as the wave packet becomes more dispersed. The process is the same as in a laser, and is sometimes called a "hazer" for hydromagnetic amplification by stimulated emission. Work by Mursula et al. (1997) casts doubt on this mechanism. Instead the authors propose that it is more likely that lower

frequency waves modulate the plasma conditions in the equatorial plane causing periodic emissions of Pc 1 waves.

The IPDP pulsations are observed in the auroral zone soon after a substorm expansion has occurred at midnight. Protons are injected rapidly in a narrow sector of local time near midnight and subsequently drift westward. As they reach the dusk meridian they drift into the plasmasphere where the Alfvén velocity is low enough to allow cyclotron resonance with the drifting ions. The most energetic ions arrive first and, because of their high parallel velocity, are Doppler shifted to low frequencies. As time progresses, lower energies arrive and resonate at successively higher frequencies. In a dynamic spectrum the signal rises in frequency from about 0.1 Hz to as high as 1 Hz over a period of about 20 min.

4.2 Drift and bounce resonances

An important internal source of ULF waves is the drift-bounce resonance mechanism. This instability allows particle distributions to give up some of their energy through the generation of waves (Southwood and Kivelson, 1982). The nature of the interaction responsible for this instability is illustrated in Figure 23. The figure displays a flat projection of an azimuthal shell of dipole field lines. The field lines have been straightened so the northern

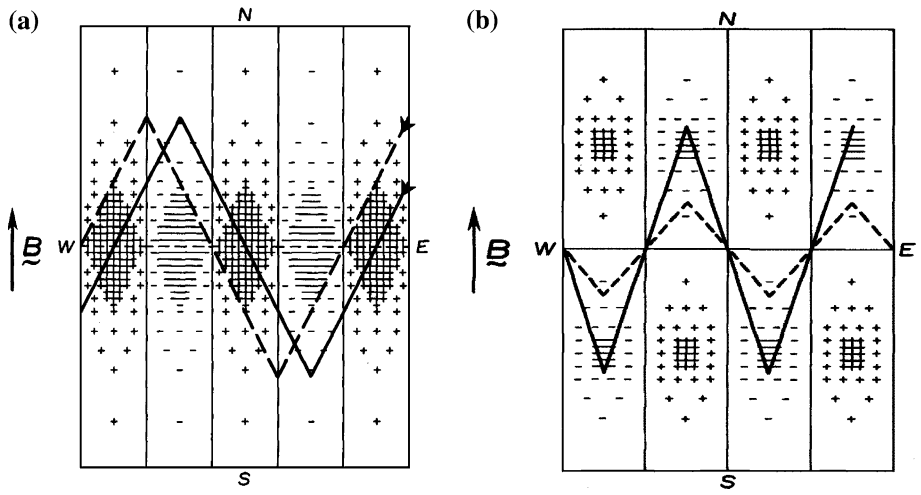

Figure 23. The azimuthal electric field of a wave is shown in the rest frame of the wave (Southwood and Kivelson, 1982). The wave is standing along the field (N–S) but is propagating azimuthally westward (W–E). (a) depicts a fundamental harmonic with maximum field at the equator while (b) shows a second harmonic. Solid lines are the trajectories of ions bouncing between mirror points at the ends of the field lines and drifting westward across the phase fronts of the wave (Reproduced by permission of American Geophysical Union).

ionosphere is at the top and the southern ionosphere at the bottom; West is to the left and East to the right. In panel (a) the plus signs show the sign of the azimuthal electric field of a fundamental mode wave standing along the field and propagating westward with a wavelength short compared to the distance around the drift shell. Plus signs indicate an eastward electric field and a minus signs westward field. The diagram is moving westward with the azimuthal phase velocity of the wave so that the wave field does not appear to change with time. However, at a fixed point in the Earth's magnetic field the diagram will sweep from right to left across an observer causing the electric field to oscillate. For the situation illustrated the magnetic perturbation is radial. Normally this would be the fast mode wave, but it can be shown that the assumption of a short azimuthal wavelength allows one to neglect the compressional component and treat the disturbance as an Alfvén wave.

The solid and dashed lines represent the trajectories of two ions drifting westward as they bounce between mirror points in the North and South. The trajectories represent ions of a specific equatorial pitch angle and energy chosen so that they complete one full bounce (N–S–N) in the moving frame in exactly two wavelengths. The solid line represents an ion that happens to pass through the center of the eastward electric field at its most intense point. During this time the ion $\boldsymbol{E} \times \boldsymbol{B}_0$ drifts radially outward, losing energy due to inductive effects in the main field $\boldsymbol{B}_0$. As this ion approaches the mirror points it encounters westward electric field and drifts inward, gaining energy. However, since the electric field of the fundamental is weaker at the mirror points than at the equator, the ion gains less energy than it loses. Thus the ion moves outward and its energy decreases with time. The energy lost by the ion is given to the wave.

The dashed trajectory shows an ion which is a quarter wavelength ahead of the first ion. It passes through the equatorial node of the wave and experiences a weak eastward electric field at one mirror point and a weak westward field at the other. The radial motion averages to zero for this ion, and it neither gains nor loses energy. An ion starting a quarter wavelength still later will move inward and gain energy on each bounce, damping the wave. If the ions are not bunched in azimuth, and there are equal numbers inside and outside the drift shell, then the net effect will be no change in the wave or particles. However, if there are more particles close to the Earth than further out, the waves will cause a net outward diffusion and the waves will gain energy from the particles. This process is the drift-bounce instability and it is a major source of ULF waves in the magnetosphere.

Figure 23b shows the situation for a second harmonic bounce resonance. For even harmonics the equator is a node of the electric field, and peaks in the electric field appear above and below the equator with opposite polarity in the two hemispheres. For this case the resonance requirement in the rest frame of the wave is that the ion drifts one azimuthal wavelength in one

bounce. The ion trajectory shown by the solid line has a small equatorial pitch angle and will sample the large westward fields at successive mirror points. This ion will experience a net inward drift due to the electric field and will gain energy. The ion shown by a dashed line has a larger equatorial pitch angle and hence a mirror point closer to the equator. It will experience weaker electric fields and not drift as far, nor gain as much energy, as a small pitch angle particle does. Again, whether the waves grow or damp depends on the radial distribution of the ions.

The drift-bounce resonance condition can be formulated mathematically quite simply. We suppose the wavelength λ is such that m cycles of the wave fit in a circular shell of radius r around the Earth. Then $\lambda = 2\pi\ r/m$. The azimuthal phase velocity of the wave is the ratio of the wavelength to period $v_\phi = \lambda/T = \lambda f = \lambda(\omega/2\pi) = r\omega/m$. Now transform to the rest frame of the wave. The drift velocity of the ion in the wave frame is $v' = r\dot{\varphi}$, where $\dot{\varphi}$ is its angular velocity. Then $v' = v_d = v_\phi$; substituting we obtain $\dot{\varphi} = \tilde{\omega}_d - \omega/m$ where $\tilde{\omega}_d$ is the ion angular drift velocity in the Earth's frame. The condition for fundamental bounce resonance can then be written as the ion bounce time equals the time to drift two wavelengths in the rest frame of the wave; thus $T_b = T_{2\lambda}$. The bounce period is given by $T_b = 2\pi/\omega_b$, where ω_b is the angular bounce frequency. The time to drift 2λ in the wave frame is given by $T_{2\lambda} = 2\pi/v' = 2(2\pi r/m)/(r\dot{\varphi}) = 4\pi/m\dot{\varphi}$. Equating and simplifying, we obtain $m\dot{\varphi} = 2\omega_b$. Transforming back to the Earth's frame by substituting for $\dot{\varphi}$, we find that $\omega - m\tilde{\omega}_d = -2\omega_b$.

The formula for the second harmonic resonance differs by only a factor of two on the right hand side. Both situations are special cases of the general resonance formula $\omega - m\tilde{\omega}_d = N\omega_b$, where N is a positive or negative integer. Clearly there is a wide variety of possible drift-bounce resonances.

4.3 Earthward directed plasma flows

Another source of waves in the magnetosphere are the Earthward directed flows that occur in the plasma sheet during substorms. Apparently, these flows are created by bursts of magnetic reconnection at an X-line in the tail. The flows are transient with durations of a few minutes and localized in azimuth to a few Earth radii. The flows transport plasma and magnetic field Earthward. As they approach the Earth (8–15 Re), the pressure gradients in the midnight region slow the flow and divert it around the Earth. As soon as these flows are created the channel becomes polarized in exactly the manner described earlier for the creation of Alfvén waves. The duskward pointing electric field produced by this polarization is propagated to the ionosphere by an Alfvén wave. In the ionosphere the electric field drives a westward current. The $\boldsymbol{J} \times \boldsymbol{B}$ force exerted on the ionosphere by this current accelerates the ionospheric plasma equatorward. Because of inertia the

ionosphere does not move as fast as the electric field would expect so the wave is reflected, reducing the total electric field. The wave reverberates between the equator and the ionosphere several times. The signal measured on the ground has the form of a short train of waves with a duration of about 10 min and a period of about 100 s. These are called Pi 2 bursts. These ULF waves are always associated with the onset of substorms, pseudo breakups, and intensifications of an ongoing substorm. An example taken from the work of Kepko et al. (2001) is shown in Figure 24. This correlation suggests that bursty flows play an essential role in the generation of substorms.

When the Earthward flow bursts impact the inner magnetosphere they radiate compressional waves that travel across the field lines and eventually

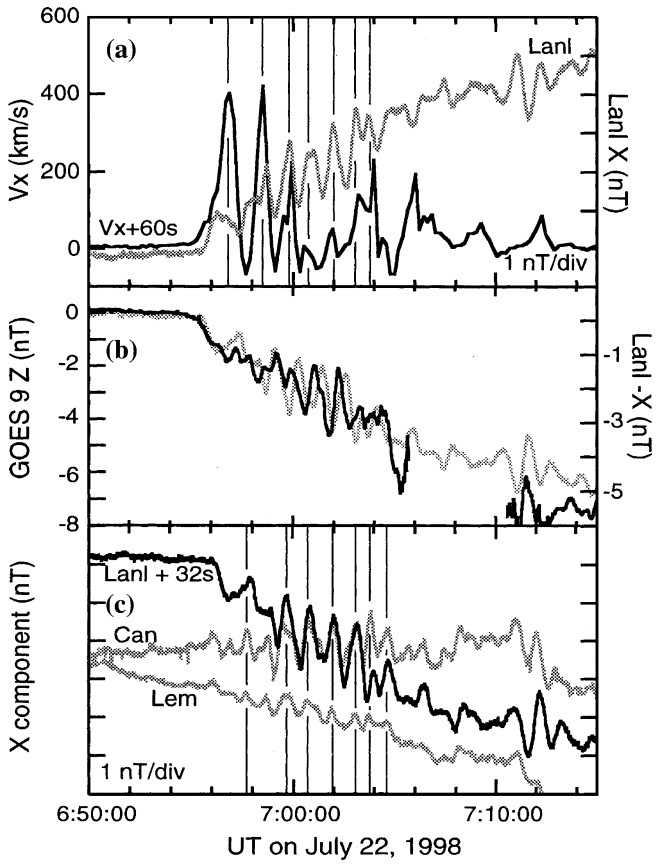

Figure 24. A comparison of the X component of flow at Geotail with the LANL magnetometer H component, showing the relation of Pi 2 pulses to pulses in the flow. The sign of the LANL data has been reversed in the middle and bottom panels for easier comparison. The same Pi 2 was seen at the synchronous satellite GOES-9 and at other ground stations (Reproduced by permission of American Geophysical Union, Kepko et al., 2001).

couple to field line resonances. The bursty flows are often structured with periods of order 100 s caused by unknown processes in the tail. The periodicity associated with the peaks in flow can structure the spectrum of compressional waves that eventually couple to Alfvén waves. The velocity shear between the edges of these flow channels and stationary plasma may generate Kelvin–Helmholtz waves. Sometimes the distribution of plasma pressure and the field line curvature become favorable to the growth of the interchange instability or the ballooning mode.

4.4 Modulation of the auroral electrojet

Another source of ULF wave activity at high latitudes on the night side is charged particle precipitation. As discussed above, the cyclotron instability can scatter particles into the atmosphere causing aurora, and creating waves. When electrons are involved, it is the electron cyclotron frequency and VLF waves ($\sim$1836 times higher frequency, $\sim$kHz) that are created. The impact of these particles on the ionosphere increases the conductivity and alters the strength and direction of the auroral electrojets. These changes in current cause magnetic variations on the ground that are indistinguishable from those of ULF waves. An example of this mechanism is Ps 6 pulsations (pulsations substorm).

Ps 6 are fluctuations with periods of 10–40 min. They are seen primarily in the East component in the post midnight sector during the recovery phase of substorms and during steady magnetospheric convection. They are associated with auroral torches or omega bands (Robinson et al., 1995). Torches are tongues of auroral luminosity that drift eastward from midnight towards dawn. The torches are rooted at the equatorward edge of the auroral zone and project poleward towards a second band of luminosity at the poleward edge of the oval. The dark regions between torches are called omega bands because the dark regions have the shape of inverted letter omega. The magnetic fluctuations are caused by a diversion of the electrojet into a field-aligned current system (Amm, 1996). Current comes down into the poleward portion of the tongue and exits near the equatorward edge. A southward directed current in the ionosphere creates East–West fluctuations on the ground. The cause of the torches is not known.

5. Conclusions

The scientific study of micropulsations, magnetic pulsations, and ULF waves has a long history. Modern instruments and satellite observations have revealed a very complex taxonomy of hydromagnetic waves that reach the Earth's surface. These waves are generated by processes as far away as the

Sun and as close as the ionosphere. There are many sources of waves both external and internal to the magnetosphere. The magnetosphere itself is a resonant cavity and a waveguide for waves that propagate through the system. These cavities respond to broadband sources by resonating at discrete frequencies. These cavity modes couple to field line resonances that drive currents in the ionosphere. These currents reradiate the energy as electromagnetic waves that propagate to the ground. Because of these resonances there are very rapid variations in wave phase at the Earth's surface. It is almost never correct to assume that plane ULF waves are incident on the Earth from outer space.

Many of the waves now have accepted explanations in terms of physical processes in the solar wind or magnetosphere. Knowledge of the wave characteristics and the current state of space weather can give us a good idea of what waves are likely to be occurring at any particular latitude and local time. The waves are diagnostic of the conditions in space. Measurements on the ground can be used to perform remote sensing of the conditions in the magnetosphere and solar wind. They can also be used to probe the subsurface conductivity structure of the Earth.

Acknowledgements

The author would like to acknowledge support for this work derived from several grants, including NSF ATM 98-19935, NSF ATM 99-72069, and Los Alamos National Laboratory LANL #1001R. He also thanks Dr. R. Clauer, Dr. M. Kivelson, Dr. A. Ridley, and Dr. C. Waters for help in understanding their earlier work.

References

Alfvén, H., and Falthammar, C.-G.: 1963, *Cosmical Electrodynamics: Fundamental Principles*, Clarendon Press, Oxford 228.

Allan, W., Manuel, J. R., and Poulter, E. M.: 1991. 'Magnetospheric Cavity Modes: Some Nonlinear Effects', *J. Geophys. Res.* **96**(A7), 11461–11473.

Amm, O.: 1996. 'Improved Electrodynamic Modeling of an Omega Band and Analysis of its Current System', *J. Geophys. Res.* **101**(A2), 2677–2683.

Baker, D. N., Pulkkinen, T. I., Angelopulos, V., Baumjohann, W., and McPherron, R. L.: 1996. 'Neutral Line Model of Substorms: Past Results and Present View', *J. Geophys. Res.* **101**(A6), 12875–13010.

Baumjohann, W., and Treumann, R. A.: 1996, *Basic Space Plasma Physics*, Imperial College Press, London 329 pp.

Belcher, J. W., and Davis, L. Jr.: 1971. 'Large-amplitude Alfvén Waves in the Interplanetary Medium. II', *J. Geophys. Res.* **76**(16), 3534–3563.

Birn, J., and Hesse, M.: 1996. 'Details of Current Disruption and Diversion in Simulations of Magnetotail Dynamics', *J. Geophys. Res.* **101**(A7), 15345–15358.

Brice, N.: 1964. 'Fundamentals of Very Low Frequency Emission Generation Mechanisms', *J. Geophys. Res.* **69**(21), 4515–4522.

Chapman, S., and Bartels, J.: 1962, *Geomagnetism*,Vol. 1, Clarendon Press, Oxford.

Chi, P., and Russell, C. T.: 2001. 'Two Methods Using Magnetometer-array Data for Studying Magnetic Pulsations', *Terrest. Atmos. Oceanic Sci.* **12**(4), 649–662.

Cornwall, J. M.: 1965. 'Cyclotron Instabilities and Electromagnetic Emissions in the Ultra Low Frequency and Velry Low Frequency Ranges', *J. Geophys. Res.* **70**(1), 61–69.

Crowley, G., Hughes, W. J., and Jones, T. B.: 1987. 'Observational Evidence of Cavity Modes in the Earth's Magnetosphere', *J. Geophys. Res.* **92**(A11), 12233–12240.

Ding, D. Q., Denton, R. E., Hudson, M. K., and Lysak, R. L.: 1995. 'An MHD Simulation Study of the Poloidal Mode Field Line Resonance in the Earth's Dipole Magnetosphere', *J. Geophys. Res.* **100**(A1), 63–77.

Engebretson, M., Zanetti, L. J., Potemra, T. A., Baumjohann, W., Luhr, H., and Acuna, M. H.: 1987. 'Simultaneous Observation of Pc3–4 Pulsations in the Solar Wind and in the Earth's Magnetosphere', *J. Geophys. Res.* **92**, 10053.

Engebretson, M. J., Lin, N., Baumjohann, W., Luehr, H., Anderson, B. J., Zanetti, L. J., Potemra, T. A., McPherron, R. L., and Kivelson, M. G.: 1991. 'A Comparison of ULF Fluctuations in the Solar Wind Magnetosheath, and Dayside Magnetosphere. 1. Magnetosheath Morphology', *J. Geophys. Res.* **96**(A3), 3441–3454.

Fukushima, N.: 1969. 'Equivalence in Ground Geomagnetic Effect of Chapman–Vestine's and Birkeland–Alfvén's Electric Current System for Polar Magentic Subtorms', *Rep. Ionos. Space Res. Jpn.* **23**, 219–227.

Gonzalez, W. D., Joselyn, J. A., Kamide, Y., Kroehl, H. W., Rostoker, G., Tsurutani, B. T., and Vasyliunas, V. M.: 1994. 'What is a Geomagnetic Storm?', *J. Geophys. Res.* **99**(A4), 5771–5792.

Greenstadt, E. W.: 1984. 'Oblique, Parallel, and Quasi-Parallel Morphology of Collisionless Shocks in the Heliosphere: Review of Current Research', in B. T. Tsurutani, and R. G. Stone (eds.), *Geophysical Monograph 35.*, American geophysical Union, Washington, DC, U.S.A., pp. 169–184.

Greenstadt, E. W. and Fredericks, R. W.: 1979, 'Shock Systems in Collisionless Space Plasmas', in L.J. Lanzerotti, C.F. Kennel, and E.N. Parker (eds.), *Solar System Plasma Physics*, North-Holland Publishing Co.

Greenstadt, E. W., Mellott, M. M., McPherron, R. L., Russell, C. T., Singer, H. J., and Knecht, D. J.: 1983. 'Transfer of Pulsation-related Wave Activity across the Magnetopause Observations of Corresponding Spectra by ISEE-1 and ISEE-2', *Geophys. Res. Lett.* **10**(8), 659–662.

Greenstadt, E. W., Olson, J. V., Loewen, P. D., Singer, H. J., and Russell, C. T.: 1979a. 'Correlation of Pc 3, 4, and 5 Activity with Solar Wind Speed', *J. Geophys. Res.* **84**(A11), 6694–6696.

Greenstadt, E. W., Singer, H. J., Russell, C. T., and Olson, J. V.: 1979b. 'IMF Orientation, Solar Wind Velocity, and Pc 3–4 Signals: A Joint Distribution', *J. Geophys. Res.* **84**(A2), 527–532.

Hoppe, M. M., Russell, C. T., Eastman, T. E., and Frank, L. A.: 1982. 'Characteristics of the ULF Waves Associated with Upstream Ion Beams', *J. Geophys. Res.* **87**(A2), 643–650.

Hughes, W. J.: 1974. 'The Effect of the Atmosphere and Ionosphere on Long Period Magnetospheric Micropulsations', *Planet. Space Sci.* **22**, 1157.

Hughes, W. J.: 1983. 'Hydromagnetic Waves in the Magnetosphere', in R. L. A. F. Carovillano and J.M. Forbs (eds.), *Solar-Terrestrial Physics: Principles and Theoretical Foundations*, D. Reidel Publishing Company, Dordrecht, pp. 453–477.

Jacobs, J. A., Kato, Y., Matsushita, S., and Troitskaya, V. A.: 1964. 'Classification of Geomagnetic Micropulsatiions', *J. Geophys. Res.* **69**(1), 180–181.

Keller, K. A., and Lysak, R. L.: 2001. 'MHD Simulation of Magnetospheric Waveguide Modes', *J. Geophys. Res.* **106**(A5), 8447–8454.

Kepko, L., Kivelson, M. G., and Yumoto, K.: 2001. 'Flow Bursts, Braking, and Pi2 Pulsations', *J. Geophys. Res.* **106**(A2), 1903–1915.

Kepko, L., Spence, H. E., and Singer, H.: 2002, ULF Waves in the Solar Wind as Direct Drivers of Magnetospheric Pulsations', *Geophys. Res. Lett.* 29(8).

Kivelson, M., and Southwood, D. J.: 1991. 'Ionospheric Traveling Vortex Generation by Solar Wind Buffeting of the Magnetosphere', *J. Geophys. Res.* **96**(A2), 1661–1667.

Kivelson, M. G., Cao, M., McPherron, R. L., and Walker, R. J.: 1997. 'A possible signature of magnetic cavity mode oscillations in ISEE spacecraft oscillations', *J. Geomag. Geoelectr.* **49**, 1079–1098.

Kivelson, M. G., Etcheto, J., and Trotignon, J. G.: 1984. 'Global Compressional Oscillations of the Terrestrial Magnetosphere: The Evidence and a Model', *J. Geophys. Res.* **89**(11), 9851–9856.

Lee, D. H., and Lysak, R. L.: 1989. 'Magnetospheric ULF Wave Coupling in the Dipole Model: The Impulsive Excitation', *J. Geophys. Res.* **94**(A12), 17097–17103 + 3 plates.

Lee, D. H., and Lysak, R. L.: 1991. 'Monochromatic ULF Wave Excitation in the Dipole Magnetosphere', *J. Geophys. Res.* **96**(A4), 5811–5817.

Liemohn, M. W., Kozyra, J. U., Thomsen, M .F., Roeder, J. L., Lu, G., Borovsky, J. E., and Cayton, T. E.: 2001. 'Dominant Role of the Asymmetric Ring Current in Producing the Stormtime Dst*', *J. Geophys. Res.* **106**(A6), 10883–10904.

Lin, N .M. J. E., Anderson, B. J., McPherron, R. L., Kivelson, M. G., Baumjohann, W., Luehr, H., Potemera, T. A., and Zanetti, L. J.: 1991. 'A Comparison of ULF Wave Fluctuations in the Solar Wind, Magnetosheath, and Dayside Magnetosphere, 2. Field and Plasma Conditions in the Magnetosheath', *J. Geophys. Res.* **96**(A3), 3455–3464.

Lysak, R. L.: 1988. 'Theory of Auroral Zone PiB Pulsation Spectra', *J. Geophys. Res.* **93**(A6), 5942–5946.

Mann, I. R., Wright, A. N., and Cally, P. S.: 1995. 'Coupling of Magnetospheric Cavity Modes to Field Line Resonances: A Study of Resonance Widths', *J. Geophys. Res.* **100**(A10), 19441–19456.

McHenry, M. A., Clauer, C. R., Friis-Christensen, E., Newell, P. T., and Kelly, J. D.: 1990. 'Ground Observations of Magnetospheric Boundary Layer Phenomena', *J. Geophys. Res.* **95**(A9), 14995–15005.

McPherron, R. L.: 1991. 'Physical Processes Producing Magnetospheric Substorms and Magnetic Storms', in J. Jacobs (ed.), *Geomagnetism*, Academic Press, London, pp. 593–739.

McPherron, R. L., Russell, C. T., and Aubry, M.: 1973. 'Satellite Studies of Magnetospheric Substorms on August 15, 1978, 9. Phenomenological Model for Substorms', *J. Geophys. Res.* **78**(16), 3131–3149.

Mursula, K., Rasinkangas, R., Bosinger, T., Erlandson, R. E., and Lindqvist, P. A.: 1997. 'Nonbouncing Pc 1 Wave Bursts', *J. Geophys. Res.* **102**(A8), 17611–17624.

Nagai, T., and Machida, S.: 1998. 'Magnetic Reconnection in the Near-Earth Magnetotail', in A. Nishida, D. N. Baker, and S. W. H. Cowley (eds.), *New Perspectives on the EArth's Magnetotail*, American Geophysical Union, Washington, DC, pp. 211–224.

Pilipenko, V. A., Fedorov, E. N., and Engebretson, M. J.: 2002. 'Alfvén Resonator in the Topside Ionosphere Beneath the Auroral Acceleration Region', *J. Geophys. Res.* **107**(A9), SMP 21–1-SMP 21–10doi:10.1029/2002JA009282.

Radoski, H. R.: 1971. 'A Note on the Problem of Hydromagnetic Resonances in the Magnetosphere', *Planet. Space Sci.* **19**, 1012.

Rankin, R., Frycz, P., Tikhonchuk, V. T., and Samson, J. C.: 1995. 'Ponderomotive Saturation of Magnetospheric Field Line Resonances', *Geophys. Res. Lett.* **22**(13), 1741–1744.

Rickard, G. J., and Wright, A. N.: 1995. 'ULF Pulsations in a Magnetospheric Waveguide: Comparison of Real and Simulated Satellite Data', *J. Geophys. Res.* **100**(A3), 3531–3537.

Ridley, A. J., Moretto, T., Ernstrom, P., and Clauer, C. R.: 1998. 'Global Analysis of Three Traveling Vortex Events during the November 1993 Storm using the Assimilative Mapping of Ionospheric Electrodynamics Technique', *J. Geophys. Res.* **103**(A11), 26349–26358.

Robinson, R. M., Chenette, D. L., Datlowe, D. W., Schumaker, T. L., Vondrak, R. R., Bythrow, P. F., Potemra, T. A., Sharber, J. R., and Winningham, J. D.: 1995. 'Field-aligned Currents Associated with Spatially Periodic X-ray Structures in the Morningside Auroral Oval', *J. Geophys. Res.* **100**(A12), 23945–23952.

Russell, C. T.: 1985. 'Planetary Bow Shock', in R. G. Stone (ed.), *Collisionless Shocks in the Heliosphere: Reviews of Current Research*, American Geophysical Union, Washington, D.C., pp. 109–130.

Russell, C. T., and Fleming, B. K.: 1976. 'Magnetic Pulsations as a Probe of the Interplanetary Magnetic Field: A Test of the Borok B index', *J. Geophys. Res.* **81**(34), 5882–5886.

Russell, C. T., and Hoppe, M. M.: 1983. 'Upstream Waves and Particles', *Space Sci. Rev.* **34**(2), 155–172.

Samson, J. C., Greenwald, R. A., Ruohoniemi, J. M., Hughes, T. J., and Wallis, D. D.: 1991. 'Magnetometer and Radar Observations of Magnetohydrodynamic Cavity Modes in the Earth's Magnetosphere', *Can. J. Phys.* **69**(8–9), 929–937.

Samson, J. C., Harrold, B. G., Ruohoniemi, J. M., Greenwald, R. A., and Walker, A. D. M.: 1992. 'Field Line Resonances Associated with MHD Waveguides in the Magnetosphere', *Geophys. Res. Lett.* **19**(5), 441–444.

Samson, J. C., Waters, C. L., Menk, F. W., and Fraser, B. J.: 1995. 'Fine Structure in the Spectra of Low Latitude Field Line Resonances', *Geophys. Res. Lett.* **22**(16), 2111–2114.

Singer, H., Russell, C. T., Kivelson, M., Greenstadt, E. W., and Olson, J.: 1977. 'Evidence for the Control of Pc 3,4 Magnetic Pulsations by the Solar Wind Velocity', *Geophys. Res. Lett.* **4**(9), 377–379.

Southwood, D. J.: 1974. 'Some Features of Field Line Resonances in the Magnetosphere', *Planet. Space Sci.* **22**(3), 483–491.

Southwood, D. J., and Hughes, W. J.: 1978. 'Source Induced Vertical Components in Geomagnetic Pulsation Signals', *Planet. Space Sci.* **26**, 715.

Southwood, D. J., and Hughes, W. J.: 1983. 'Theory of Hydromagnetic Waves in the Magnetosphere', *Space Sci. Rev.* **35**, 301–366.

Southwood, D. J., and Kivelson, M. G.: 1982. 'Charged Particle Behavior in Low-Frequency Geomagnetic Pulsations. II. Graphical Approach', *J. Geophys. Res.* **87**(A3), 1707–1711.

Southwood, D. J., and Kivelson, M. G.: 1990. 'The Magnetohydrodynamic Response of the Magnetospheric Cavity to Changes in Solar Wind Pressure', *J. Geophys. Res.* **95**(A3), 2301–2309.

Spreiter, J. R., and Stahara, S. S.: 1985. 'Magnetohydrodynamic and Gasdynamic Theories for Planetary Bow Waves', in R. G. Stone (ed.), *Collisionless Shocks in the Heliosphere: Reviews of Current Research*, American Geophysical Union, Washington DC, pp. 85–107.

Sugiura, M., and Wilson, C. R.: 1964. 'Oscillation of the Geomagnetic Field Lines and Associated Magnetic Perturbations at Conjugate points', *J. Geophys. Res.* **69**(7), 1211–1216.

Takahashi, K., and McPherron, R. L.: 1982. 'Harmonic Structure of Pc 3–4 Pulsations', *J. Geophys. Res.* **87**(A3), 1504–1516.

Takahashi, K., McPherron, R. L., and Greenstadt, E. W.: 1981. 'Factors Controlling the Occurrence of Pc 3 Magnetic Pulsations at Synchronous Orbit', *J. Geophys. Res.* **86**(A7), 5472–5484.

Thomsen, M. F.: 1985. 'Upstream Suprathermal Ions', in R. G. Stone (ed.), *Collisionless Shocks in the Heliosphere: Reviews of Current Research*, American Geophysical Union, Washington DC, pp. 253–270.

Vasyliunas, V. M.: 1983. 'Large-scale Morphology of the Magnetosphere', in R. L. A. F. Carovillano, and J. M. Forbs (eds.), *Solar-Terrestrial Physics: Principles and Theoretical Foundations*, D. Reidel Publishing Company, Dordrecht, pp. 243–254.

Walker, A. D. M.: 1998. 'Excitation of Magnetohydrodynamic Cavities in the Magnetosphere', *J. Atmos. Sol-Terr. Phys.* **60**(13), 1279–1293.

Walker, A. D. M., and Greenwald, R. A.: 1980. 'Pulsation Structure in the Ionosphere Derived from Auroral Radar Data', *J. Geomag. Geoelec.* **32**(suppl.2), 111–127.

Waters, C. L., Harrold, B. G., Menk, F. W., Samson, J. C., and Fraser, B. J.: 2000. 'Field Line Resonances and Waveguide Modes at Low Latitudes. 2. A Model', *J. Geophys. Res.* **105**(A4), 7763–7774.

Waters, C. L., Takahashi, K., Lee, D.-H., and Anderson, B. J.: 2002. 'Detection of Ultralow-Frequency Cavity Modes Using Spacecraft Data', *J. Geophys. Res.* **107**(A10), SMP 7-1 to 7-20doi:10.1029/2001JA000224.

Yahnin, A., and Moretto, T.: 1996. 'Travelling Convection Vortices in the Ionosphere Map to the Central Plasma Sheet', *Ann. Geophys.* **14**(10), 1025–1031.

Yumoto, K.: 1988. 'External and Internal Sources of Low-frequency MHD Waves in the Magnetosphere – A Review', *J. Geomag. Geoelec.* **40**(3), 293–311.